

Contribution to the initialization of linear non-commensurate
fractional-order systems for the joint estimation of parameters and
fractional differentiation orders

Mohamed A. Bahloul^{1,2}, Zehor Belkhatir³ and Taous-Meriem Laleg Kirati^{2,4}

¹ College of Engineering, Electrical Engineering Department at Alfaisal University,
Riyadh 11533, Saudi Arabia. E-mail: mbahloul@alfaisal.edu

² Electrical and Computer Engineering Department, KAUST, Saudi Arabia.
E-mail: mohamad.bahloul@kaust.edu.sa, taousmeriem.laleg@kaust.edu.sa

³ School of Engineering and Sustainable Development, De Montfort University,
United Kingdom, E-mail: zehor.belkhatir@dmu.ac.uk

⁴ National Institute for Research in Digital Science and Technology, Paris-Saclay, France.

October 19, 2022

Abstract

It has been recognized that using time-varying initialization functions to solve the initial value problem of fractional-order systems (FOS) is both complex and essential in defining the dynamical behavior of the states of FOSs. In this paper, we investigate the use of the initialization functions for the purpose of estimating unknown parameters of linear non-commensurate FOSs. In particular, we propose a novel "pre-initial" process that describes the dynamic characteristic of FOSs before the initial state and

consists of designing an appropriate time-varying initialization function that ensures accurate convergence of the estimates of the unknown parameters. To do so, we propose an estimation technique that consists of two steps: (i) to design of practical initialization function that is output-dependent and which is employed; (ii) to solve the joint estimation problem of both parameters and fractional differentiation orders (FDOs). A convergence proof has been presented. The performance of the proposed method is illustrated through different numerical examples. Potential applications of the algorithm to joint estimation of parameters and FDOs of the fractional arterial Windkessel and neurovascular models are also presented using both synthetic and real data. The added value of the proposed "pre-initial" process to solve the studied estimation problem is shown through different simulation tests that investigate the sensitivity of estimation results using different time-varying initialization functions.

1 Introduction

Over the past 325 years, fractional calculus (FC) has attracted the attention of mathematicians and engineers working in various fields of science and engineering [1]. FC started to be used as a powerful tool to describe and explore complicated dynamical systems of real-world applications, e.g., biology [2], control [3], economic [4]. Indeed FC can describe systems with high-order dynamics and complex nonlinear aspects employing fewer coefficients than the integer-order calculus. The arbitrary order of the derivatives provides an extra degree of freedom to concisely and precisely entail the hidden dynamics having a different origin of memory effect. A distinctive feature of fractional-order calculus is that contrary to integer-order calculus, the fractional-order one accounts for the system's memory. In fact, the fractional-order derivative depends not only on the local conditions of the evaluated time but also on the entire history of the function. This peculiarity is usually valuable when the

studied system holds a long-term "memory," and any assessed point depends on the past values of the function [5]. Accordingly, one essentially-crucial prerequisite to ensuring the fractional-order theory functioning is the adequate initialization and the proper incorporation of the history of the system [6].

Generally, the initialization of fractional-order systems is considered complicated and challenging. This dilemma surfaced notably in the case of the non-zero initial value. In fact, it is challenging to design appropriate initialization functions that guarantee the acquiring of exact states of the system while accounting for its history, [7]. The pre-initialization process and the initialization functions of non-zero initial value-based fractional-order systems remain an open and controversial question. Various effective methods have been developed to analyze the characteristic of fractional order derivatives where initial values are insufficient [8, 9, 10]. Lorenzo et al., [11] was the first to demonstrate that time-varying functions are more suitable for the initialization of fractional-order systems rather than constant ones. The time-varying initialization has a profound effect on the standard definitions of fractional-order derivative and integral. Different time-varying initialization functions may lead to the same initial value from where the fractional-order operator starts; however, as the system's dynamic is related to the pre-initial process, different initialization functions result in different responses. This fact is known as the aberration phenomenon [12]. Accordingly, designing the proper initialization function to acquire the desired convergence of the fractional differential system is deemed very problematic.

For this reason, in this report, we introduce a novel pre-initialization process that warrants a fast and precise convergence of the joint estimation of the parameters and differentiation orders of the fractional differential system (FOS). The key hypothesis in the design is to consider an output-dependent initialization function when estimating the unknowns. This will reduce the infinite-dimensional space

of initialization functions into a finite parametric space where the remaining degree of freedom is about the length of the history function to consider. In addition, we proposed a two-stage algorithm: while the first stage solves a system of linear equations to estimate the parameters of the FOS, the second stage uses the iterative first-order Newton's method [13, 14, 15, 16] to estimate the fractional differentiation orders. Our contributions are as follows: (i) we consider a time-varying function to initialize the FOS; (ii) we design a pre-initialization process based on the output signal; and (iii) we solve a simple linear equation system to estimate the parameters, and iteratively we apply Newton's method to estimate the fractional differentiation orders.

The performance of the proposed method is illustrated through different numerical examples. Additionally, potential applications of the algorithm are presented, which consists of estimating parameters and fractional differentiation orders of a fractional-order arterial Windkessel and neurovascular models. To the best to the author's knowledge, this is the first study that accounts for the initialization function as part of the parameters estimation problem for fractional differential systems.

2 Notations

For a clear perception of the report, in this section, we present the adopted notation and the basic definitions of the fractional-order integral and derivative. Through the following we consider a smooth function $f(t)$ such that $f(t)$ is zero for $t \leq t_{abs}$ and $f(t)$ is $f_{in}(t)$ for $t_{abs} \leq t \leq t_{in}$.

- ${}_{t_{in}}D_t^\alpha f(t)$ denotes the 'initialized' α^{th} order differ-integration of $f(t)$ from start point t_0 to t .
- ${}_{t_{in}}d_t^\alpha f(t)$ represents the 'non-initialized' generalized (or fractional) α^{th} order differ-integration of $f(t)$. It is equivalent to shifting the origin of function $f(t)$ at the start of the point from

where differ-integration starts.

$$\frac{d^\alpha f(t)}{[d(t-t_{in})^\alpha]} \equiv {}_{t_{in}}d_t^\alpha f(t). \quad (1)$$

- Ψ denotes the time-varying initialization function or history function. It is also known as the complementary function [17]. The expression between initialized differ-integral and non-initialized ones is:

$${}_{t_{in}}D_t^\alpha f(t) = {}_{t_{in}}d_t^\alpha f(t) + \Psi(f, \alpha, t_{abs}, t_{in}, t) \quad (2)$$

2.1 Definitions

There are many kinds of definitions for fractional-order differ-integration. Here we present the more commonly known ones, namely the *Riemann-Liouville*, *Caputo* and *Grunwald-Letnikov* definitions. A detailed note on the different definitions might be found in this reference, [11, 17].

Definition 1. *The Riemann-Liouville (R-L) definition of fractional-order integration is drawn as:*

$${}_{t_{in}}^{RL}d_t^{-\alpha} f(t) = \frac{1}{\Gamma(\alpha)} \int_{t_{in}}^t \frac{f(\tau)}{(t-\tau)^\alpha} d\tau, \quad (3)$$

here t_{abs} is noted as the terminal point as well. $0 < \alpha < 1$ and $\Gamma(x)$ corresponds to so-called Gamma-function, written as $\Gamma(x) = \int_0^\infty e^{-u} u^{x-1} du$.

Definition 2. *The R-L definition of fractional-order derivative is based on the above definition (3) and the standard integer-order derivative:*

$${}_{t_{in}}^{RL}d_t^\alpha f(t) = \frac{d}{dt} \left[{}_{t_{in}}d_t^{-(1-\alpha)} f(t) \right]. \quad (4)$$

Definition 3. *The Caputo definition of fractional-order differentiation takes the integer-order differentiation of the function first and then takes a fractional-order integration:*

$${}_{t_{in}}^C d_t^\alpha f(t) = \frac{1}{\Gamma(n-\alpha)} \int_{t_{in}}^t (1-\tau)^{-\alpha-1+n} \frac{d^n}{dt^n} f(\tau) d\tau. \quad (5)$$

Definition 4. The Grunwald-Letnikov based Fractional-order differ-integration G-L defines the fractional integration and differentiation in a unified way:

$${}_{t_{in}}^{GL}d_t^\alpha f(t) = \lim_{h \rightarrow 0} h^{-\alpha} \sum_{j=0}^{\lfloor \frac{t-t_{in}}{T_s} \rfloor} (-1)^j \binom{\alpha}{j} f(t-jh), \quad (6)$$

where h is the sampling time, $\binom{\alpha}{j} = \frac{\Gamma(\alpha+1)}{\Gamma(j+1)\Gamma(\alpha-j+1)}$ and $\lfloor \cdot \rfloor$ describes the floor function and denotes the biggest integer smaller or equal to the argument.

Remark 1. Suppose $f \in C^{\lfloor \alpha \rfloor + 1}$, the G-L derivative is equivalent to the R-L derivative (see [18]).

2.2 Aberration phenomenon

This section focuses on the proposition of the so-called aberration phenomena that represent the effect of the pre-initial processes on a fractional-order system's response. To do so, we simulate a simple system that model the internal force of an axially loaded viscoelastic bar, [19]. In the following illustration example, $u(t)$ is the input denoting the longitudinal force, and $y(t)$ is the output representing the elongation. They satisfy the following fractional-order relationship:

$${}_{t_0}D_t^{0.5}y(t) = u(t) \quad (7)$$

Assume the force $u(t)$, the input of the system, is zero before the absolute zero instant of the system, and the initial instant is taken as $t_{in} = 5$. We excite the system by three different inputs U_0 , U_1 , and U_2 that are specified as follows:

$$U_0 \begin{cases} 0, & t \leq 0 \\ 0, & 0 < t < 5 \\ 1, & t \geq 5 \end{cases}, \quad U_1 \begin{cases} 0, & t \leq 0 \\ t, & 0 < t < 5 \\ 1, & t \geq 5 \end{cases}, \quad U_2 \begin{cases} 0, & t \leq 0 \\ \frac{1}{4}t^4, & 0 < t < 5 \\ 1, & t \geq 5 \end{cases} \quad (8)$$

The corresponding outputs (Y_0 , Y_1 , and Y_2) along with the initialization function, as developed in the

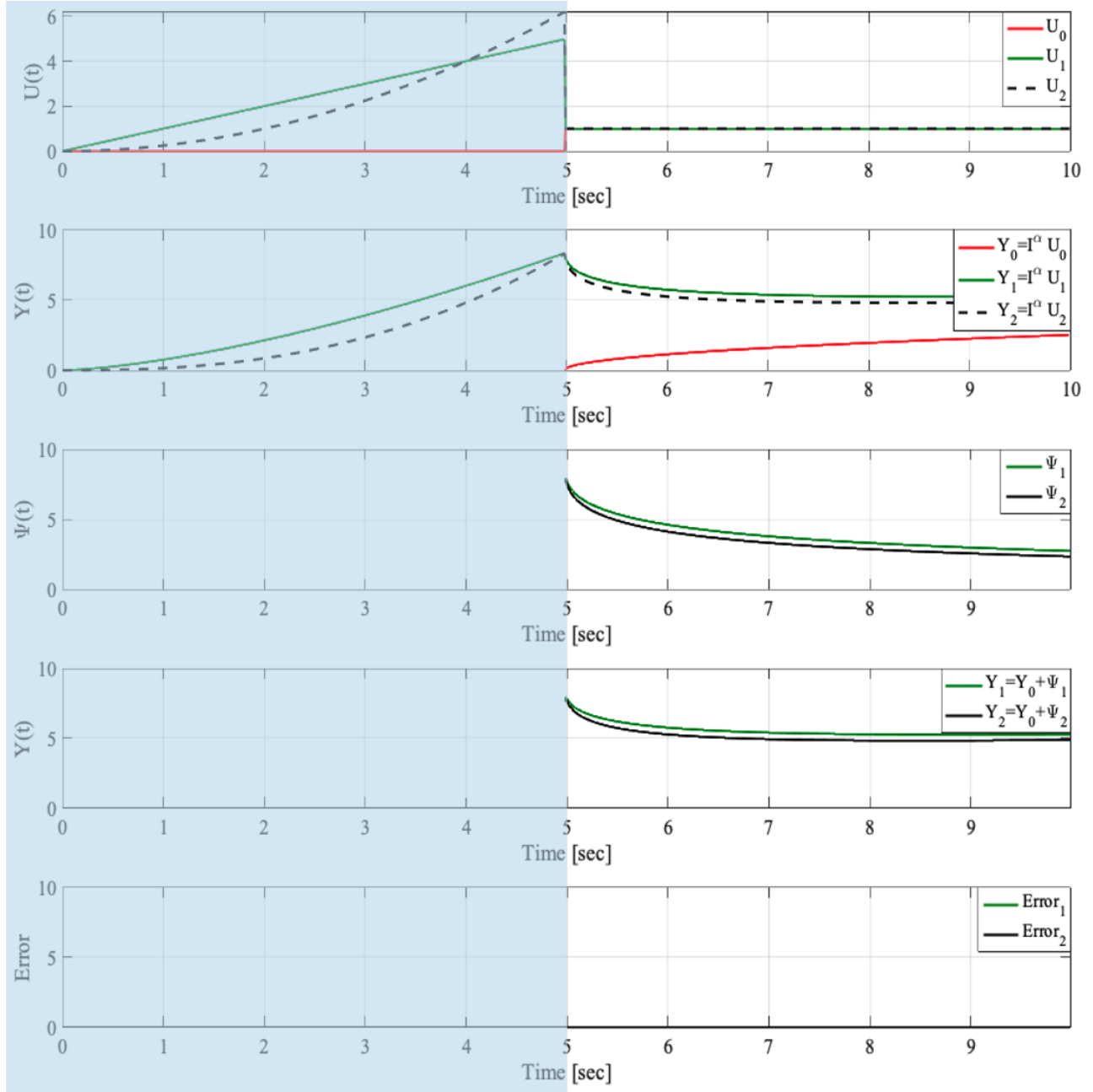


Figure 1: The aberration phenomenon.

previous section, are shown in Figure 1. It is clear from this graph that although Y_1 and Y_2 have the same values at the initial time $t_{in} = 5$ and they are excited with the same input afterward, they don't

have the same response later. In addition, from the output Y_0 that corresponds to a non-initialized response as $u(t)$ is equal to zero over the pre-initialized process $t \in [0 \ 5]$. From all these outputs, we can perceive the effect of the pre-initial process. Accordingly, in the simulation of the fractional-order system, the ignorance of infinite states at t_{in} or the improper initialization of the states before the initial instant might cause an aberration of the output. On the one hand, the noticed aberration phenomenon reflects the complexity and the difficulty of the initial value problem. On the other hand, it illustrates the great challenge of analyzing and controlling fractional-order systems. Commonly, to overcome the negative consequences of the aberration, former studies are used to transform the problems of the non-initial value into zero initial value ones. Hence, it is essential to seek the inner essence of this aspect. Furthermore, it is primordial to provide adapted procedures to select the exact time-varying history function that leads to the correct response and accurate estimation of the system's states.

2.3 Time-varying function based-initialization of FOS

The main idea of the history function based-initialization is that the initialization time-varying function $\Psi(t)$ should bring out the past history. Otherwise stated, the history function entails the effect of fractionally integrating the function from its birth [17, 15].

Assume that $f(t)$ was born at $t = t_{abs}$, that is $f(t) = 0$ for all time less than equal to t_{abs} . Then the time period between t_{abs} and t_{in} may be considered as history if the fractional-order integration starts at $t = t_{in}$ and $f(t) = f_{in}(t) \forall t \in [t_{abs} \ t_{in}]$. The fundamental idea is that the fractional-order integral $({}_{t_{in}}d_t^{-\alpha} f(t))$, should be properly initialized so that it should function as continuation of integral starting at $t = t_{abs}$. Hence an initialization function, Ψ must be added to $({}_{t_{in}}d_t^{-\alpha} f(t))$, so that the fractional-order integral starting at $t = t_{in}$ should be identical to the result starting at $t = t_{abs}$ for

$t \geq t_{in}$. The history function Ψ has the effect of allowing the function $f(t)$ and its derivatives to start at a value other than t_{in} , namely ${}_{t_{abs}}D_{t_{in}}^{-\alpha}f(t)|_{t=t_{in}}$, and continues to contribute to differ-integral response after $t = t_{in}$. That is, a function of time is added to the uninitialized integral, (not just a constant at $t = t_{in}$). The above argument can be formulated as follows: for $t > t_{in}$

$$\Psi(f_{in}, \alpha, t_{abs}, t_{in}, t) = {}_{t_{abs}}d_t^{-\alpha}f(t) - {}_{t_{in}}d_t^{-\alpha}f(t). \quad (9)$$

Generally, we differentiate two types of initialization:

- **Side-initialization:** Fully arbitrary initialization may be applied to the differ-integral operator at time $t = t_{in}$.
- **Terminal initialization:** It is assumed that the differ-integral operator can be initialized (charged) by effectively differ-integrating prior to the start time, $t = t_{in}$.

Figure 2 demonstrates the concept of initialization as a block diagram of a signal flow graph.

2.3.1 History-function based-initialization of fractional-order integration

Assume, the fractional-order integration of a function $f(t)$ starts at $t = c$ and takes place for all $t > t_{in} \geq t_{abs}$. The initialization process takes place during the period $t \in [t_{abs}, t_{in}]$. Generally the *Riemann-Liouville* (*R-L*) definition is admitted in the case where the differintegrand $f(t) = 0$ for all $t \leq t_{abs}$. The fractional-order integration based *R-L* definition of $f(t)$ is:

$${}_{t_{abs}}D_t^{-\alpha}f(t) = {}_{t_{abs}}d_t^{-\alpha}f(t) = \frac{1}{\Gamma(\alpha)} \int_{t_{abs}}^t (t - \tau)^{\alpha-1} f(\tau) d\tau, \quad (10)$$

where $(\alpha \geq 0$ and $t > t_{abs}$ subject to $f(t) = 0$ for all $t \leq t_{abs}$. $\Psi(f, -\alpha, t_{abs}, t_{abs}, t) = 0$

The following definition of fractional-order integration will apply generally (at any $t > c$):

$${}_cD_t^{-\alpha}f(t) = \frac{1}{\Gamma(\alpha)} \int_c^t (t - \tau)^{\alpha-1} f(\tau) d\tau + \Psi(f, -\alpha, a, c, t) \quad (11)$$

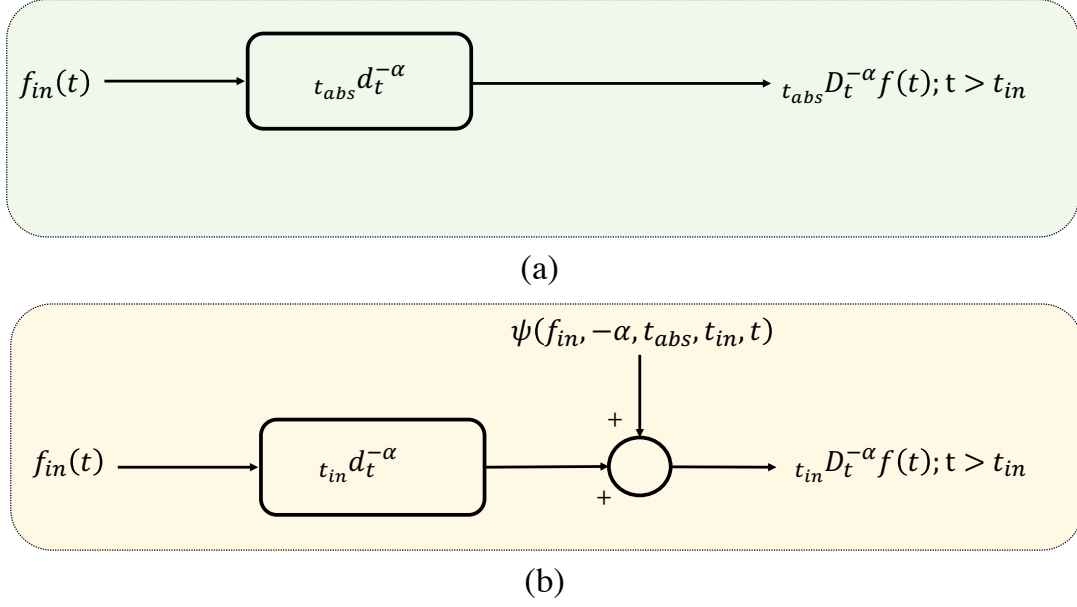


Figure 2: Signal flow graph for demonstrating initialization of fractional integration [17]. (a) illustrates the Side-initialization and (b) Terminal initialization

where $(\alpha \geq 0, t > t_{abs}, t_{in} > t_{abs}$ and $f(t) = 0$ for all $t \leq t_{abs}$.

The function $\Psi(f, -\alpha, t_{abs}, t_{in}, t)$ is called the initialization function and will be chosen such that

$${}_{t_{abs}}D_t^{-\alpha} f(t) = {}_{t_{in}}D_t^{-\alpha} f(t), \quad t > t_{in} \quad (12)$$

The above condition gives:

$$\frac{1}{\Gamma(\alpha)} \int_{t_{abs}}^t (t-\tau)^{\alpha-1} f(\tau) d\tau = \frac{1}{\Gamma(\alpha)} \int_{t_{in}}^t (t-\tau)^{\alpha-1} f(\tau) d\tau + \Psi(f, -\alpha, t_{abs}, t_{in}, t) \quad (13)$$

Hence

$$\Psi(f, -\alpha, t_{abs}, t_{in}, t) = \frac{1}{\Gamma(\alpha)} \int_{t_{abs}}^t (t-\tau)^{\alpha-1} f(\tau) d\tau - \frac{1}{\Gamma(\alpha)} \int_{t_{in}}^t (t-\tau)^{\alpha-1} f(\tau) d\tau \quad (14)$$

Since $\int_{t_{abs}}^t g(\tau) d\tau = \int_{t_{abs}}^{t_{in}} g(\tau) d\tau + \int_{t_{in}}^t g(\tau) d\tau$ we get:

$$\Psi(f, -\alpha, t_{abs}, t_{in}, t) = {}_{t_{abs}}D_{t_{in}}^{-\alpha} = \frac{1}{\Gamma(\alpha)} \int_{t_{abs}}^{t_{in}} (t-\tau)^{\alpha-1} f(\tau) d\tau \quad (15)$$

This expression for $\Psi(t)$ gives 'terminal initialization', and also brings out in the definition of fractional integral the effect of the past 'history', namely the effect of fractionally integrating the $f(t)$ from t_{abs} to t_{in} . This effect is also called terminal charging.

2.3.2 History-function based-initialization of fractional-order derivative

Unlike the integer-order derivative that is considered a local quantity, the fractional-order derivative (FD) is a non-local operator and has a history. Furthermore, as FD contains fractional-order integration, its evaluation requires the initialization process. By considering the integer-order derivative as a particular case of the fractional-order derivative, a generalization of the integer-order derivative concept also calls for initialization. Accordingly, a generalized integer-order differentiation with initialization can be defined as:

$${}_{t_{in}}D_t^m f(t) = \frac{d^m}{dt^m} f(t) + \Psi(f, m, t_{abs}, t_{in}, t), t > t_{in} \quad (16)$$

where m is an integer corresponding to the differentiation order and $\Psi(f, m, t_{abs}, t_{in}, t)$ is the initialization function. Assume a fractional-order differentiation; $\alpha \geq 0$. A function $f(t)$ is born at $t = t_{abs}$ and before that the value is zero ($f(t) = 0$ for $t \geq t_{abs}$). $\alpha = m - \beta$ equivalently m is the integer just greater than the fractional order α , by amount β . The differentiation starts at $t > t_{in}$.

A non-initialized fractional-order derivative can be expressed as:

$${}_{t_{abs}}d_t^\alpha f(t) = {}_{t_{abs}}D_t^m {}_{t_{abs}}D_t^{-\beta} f(t) \quad (17)$$

Similar to the fractional-order integration in this case the initialization function $\Psi(f, -\beta, t_{abs}, t_{abs}, t) = 0$.

If we consider the $h(t) = {}_{t_{abs}}D_t^{-\beta} f(t)$ i.e. fractional integral of function starting at t_{abs} with initialized term $\Psi(h, m, t_{abs}, t_{abs}, t) = 0$; the initialized fractional derivative looks and defined as for $\alpha \geq 0$, $t >$

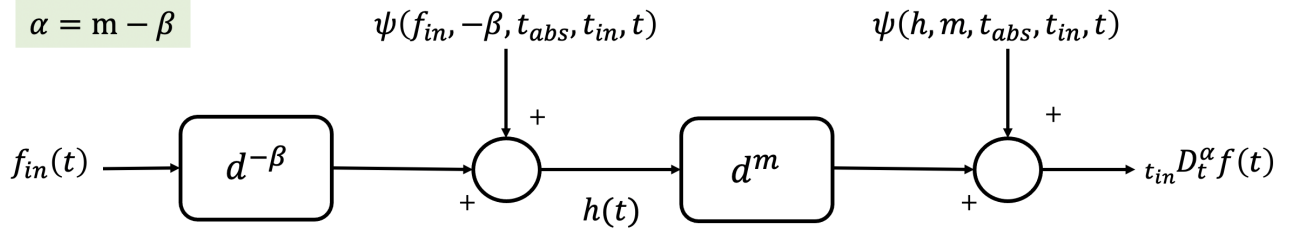


Figure 3: Initialization of fractional derivative.

$t_{in} \geq t_{abs}$.

$${}_{t_{in}}D_t^\alpha f(t) = {}_{t_{in}}D_t^m f(t) \quad {}_{t_{in}}D_t^{-\beta} f(t) \quad (18)$$

Accordingly, the history-function based-initialization of the fractional-order derivative is generally similar to that obtained with initialization of the fractional-order integral. In fact, it requires the following as the fractional-order integral:

$${}_{t_{abs}}D_t^\alpha f(t) = {}_{t_{in}}D_t^\alpha f(t) \quad (19)$$

For all $t > t_{in} \geq t_{abs}$. Specifically this requires compatibility of the derivatives starting at $t = t_{abs}$ and $t = t_{in}$ for all $t > t_{in}$.

Therefore it follows that:

$${}_{t_{in}}D_t^m \quad {}_{t_{in}}D_t^{-\beta} f(t) = {}_{t_{abs}}D_t^m \quad {}_{t_{abs}}D_t^{-\beta} f(t) \quad (20)$$

Expanding the fractional-order integrals with the initialization function introduced in the previous section we obtain:

$${}_{t_{in}}D_t^m \left(\frac{1}{\Gamma(\beta)} \int_{t_{in}}^t (t-\tau)^{\beta-1} f(\tau) d\tau + \Psi(f, -\beta, t_{abs}, t_{in}, t) \right) = \quad (21)$$

$${}_{t_{abs}}D_t^m \left(\frac{1}{\Gamma(\beta)} \int_{t_{abs}}^t (t-\tau)^{\beta-1} f(\tau) d\tau + \Psi(f, -\beta, t_{abs}, t_{abs}, t) \right)$$

For, $t > t_{in}$ and $\Psi(f, -\beta, t_{abs}, t_{abs}, t) = 0$. Using the definition of generalized integer order derivative as defined above we get:

$$\begin{aligned} \frac{d^m}{dt^m} \left\{ \frac{1}{\Gamma(\beta)} \int_{t_{in}}^t (t-\tau)^{\beta-1} f(\tau) d\tau + \Psi(f, -\beta, t_{abs}, t_{in}, t) \right\} + \Psi(h_1, m, t_{abs}, t_{in}, t) = \\ \frac{d^m}{dt^m} \frac{1}{\Gamma(\beta)} \int_{t_{abs}}^t (t-\tau)^{\beta-1} f(\tau) d\tau + \Psi(h_2, m, t_{abs}, t_{abs}, t) \end{aligned} \quad (22)$$

where $h_1 = {}_{t_{in}}D_t^{-\beta} f(t)$ and $h_2 = {}_{t_{abs}}D_t^{-\beta} f(t)$. The integer order derivative is initialized at $t = a$ thus $\Psi(h_2, m, t_{abs}, t_{abs}, t) = 0$. After rearranging the integrals we get:

$$\Psi(h_1, m, t_{abs}, t_{in}, t) = \frac{d^m}{dt^m} \left(\frac{1}{\Gamma(\beta)} \int_{t_{abs}}^{t_{in}} (t-\tau)^{\beta-1} f(\tau) d\tau - \Psi(f, -\beta, t_{abs}, t_{in}, t) \right) \quad (23)$$

The above expression is the requirement for the initialization of the derivative in general. Under the condition of terminal charging of the fractional-order integral, the initialization function of fractional integration as defined and derived earlier is:

$$\Psi(f, -\beta, t_{abs}, t_{in}, t) = \frac{1}{\Gamma(\beta)} \int_{t_{abs}}^{t_{in}} (t-\tau)^{\beta-1} f(\tau) d\tau \quad (24)$$

Hence the $\Psi(h_1, m, t_{abs}, t_{in}, t) = 0$. Figure 3 illustrates the initialization concept for fractional derivative.

2.3.3 Grunwald-Letnikov based fractional-order differ-integrals initialization concept

Definition 5. *The formulations of the time-varying history function using the most known fractional-order differ-integration definitions namely RL, C and GL can be observed in [11]. Here we present only the G-L based-one as our proposed method is based on it.*

$$\Psi_{GL}(f_{in}, \alpha, t_{in}, t_{abs}, t) = \lim_{h \rightarrow 0} \left\{ \frac{h^{-\alpha}}{\Gamma(-\alpha)} \sum_{j=0}^{N_3-1} \frac{\Gamma(N_1-1-\alpha-j)}{\Gamma(N_1-j)} f[t-(N_1-1-j)h] \right\}, \quad (25)$$

where $h = (t - t_{abs}) \setminus N_1$ is the time step, $t > t_{in} > t_{abs}$ and N_1 and N_3 are integers such that:

$$N_3 = \left(\frac{t_{in} - t_{abs}}{t - t_{abs}} \right) N_1 \quad (26)$$

3 Problem Formulation

Let us consider the following FOS:

$$y(t) + \sum_{i=1}^N a_i {}_{t_{in}} D_t^{\alpha_i} y(t) = b u(t), \quad t \in [t_{in} \ T] \quad (27)$$

where $y(t) : [t_{in} \ T] \rightarrow \mathbb{R}$ is the output, $u(t) : [t_{in} \ T] \rightarrow \mathbb{R}$ is the input. $(a_1 \ a_2 \ \dots \ a_N)$ and b are real parameters. $\alpha_i \in \wp = (n_{i-1}, n_i)$ ¹, with $n_i \in \mathbb{N}^*$ and $i = 1, 2, \dots, N$ are the fractional differentiation orders. They are assumed to be as follows: $0 \leq \alpha_1 \leq \alpha_2 \leq \dots \leq \alpha_N$, i.e., $n_i < n_{i+1}$ for $i = 1, 2, \dots, N-1$.

We substitute the initialized fractional derivative (2) in (27) which leads the following equation:

$$y(t) + \sum_{i=1}^N a_i [{}_{t_{in}} d_t^{\alpha_i} y(t) + \Psi_i(f_{in}, \alpha_i, t_{abs}, t_{in}, t)] = b u(t), \quad (28)$$

$f_{in}(t) : [t_{abs} \ t_{in}] \rightarrow \mathbb{R}$ corresponds to the history function of $y(t)$ based-initialization.

$\Psi = (\Psi_1(f_{in}, \alpha_1, t_{abs}, t_{in}, t) \ \Psi_2(f_{in}, \alpha_2, t_{abs}, t_{in}, t) \ \dots \ \Psi_N(f_{in}, \alpha_N, t_{abs}, t_{in}, t))^{tr}$ denotes the vector of initialization functions and are defined as in (9).

We denote the vectors p and α as: $p = (a_1 \ a_2 \ \dots \ a_N, b)^{tr}$, $\alpha = (\alpha_1 \ \alpha_2 \ \dots \ \alpha_N)^{tr}$ and their estimates as $\hat{p} = (\hat{a}_1 \ \hat{a}_2 \ \dots \ \hat{a}_N, \hat{b})^{tr}$ and $\hat{\alpha} = (\hat{\alpha}_1 \ \hat{\alpha}_2 \ \dots \ \hat{\alpha}_N)^{tr}$ respectively. $(\cdot)^{tr}$ denotes the transpose of the row vector.

In this work, we are interested in solving the following estimation problem (EP) that accounts for the initialized fractional-order derivative:

$$(EP) \left\{ \begin{array}{l} \text{Given the output signal } y(t) \text{ and } u(t), t \in [t_{in}, T], \text{ design a history function based-initialization,} \\ f_{in}(t), t \in [t_{abs}, t_{in}] \text{ jointly with the simultaneous estimation of the unknown parameters and} \\ \text{the fractional orders, denoted } (\hat{p}, \hat{\alpha}) \end{array} \right.$$

¹ $\wp = \prod_{i=1}^N \wp_i = \{(a_1, a_2, \dots, a_N) | \forall i = 1, 2, \dots, N, a_i \in \wp_i\}$ is the generalized Cartesian product of N sets $\wp_1, \wp_2 \dots \wp_N$.

4 Reformulation of the Estimation Problem in Discrete Space

In this section, we reformulate the initialized estimation problem in the discrete space using the Grunwald-Letnikov derivative definition given in Definition 4 and the history function based GL given in Definition 5. In the following, we present the different steps of the problem formulations:

For a given small enough sampling time h such that $h = (t - t_{abs}) \setminus N_1$,

$N_3 = (t_{in} - t_{abs} \setminus t - t_{abs}) N_1$ and $K = N_1 - N_3$. In the discrete space the system (28) can be written as follows $\forall k = 1, 2, \dots, K$

$$y(t_k) + \sum_{i=1}^N a_i [{}_{t_{in}} d_t^{\alpha_i} y(t_k) + \Psi_i(f_{in}, \alpha_i, t_{abs}, t_{in}, t_k)] = b u(t_k), \quad (29)$$

where

$$\Psi_i(f_{in}, \alpha_i, t_{in}, t_{abs}, t_k) = \frac{1}{h^{\alpha_i}} \sum_{n=0}^{N_3-1} C_n^{\alpha_i} f_{in}[t_k - (N_1 - 1 - n)h]. \quad (30)$$

where $C_j^{\alpha_i} (j = 0, 1, \dots, N_1)$ are the binomial coefficients recursively computed using the following formula:

$$C_0^{\alpha_i} = 1, \quad C_j^{\alpha_i} = \left(1 - \frac{1 + \alpha_i}{j}\right) C_{j-1}^{\alpha_i}. \quad (31)$$

Substituting (30) in (29) we obtain:

$$y(t_k) + \sum_{i=1}^N a_i \left[{}_{t_{in}} d_t^{\alpha_i} y(t_k) + \frac{1}{h^{\alpha_i}} \sum_{n=0}^{N_3-1} C_n^{\alpha_i} f_{in}[t_k - (N_1 - 1 - n)h] \right] = b u(t_k). \quad (32)$$

Based on Definition 4 and substituting ${}_{t_{in}} d_t^{\alpha_i} y(t_k)$ by its formula described in (6) we obtain the following:

$$y(t_k) + \sum_{i=1}^N a_i \left[\frac{1}{h^{\alpha_i}} \sum_{j=0}^{N_1} C_j^{\alpha_i} y(t_{k-j}) + \frac{1}{h^{\alpha_i}} \sum_{n=0}^{N_3-1} C_n^{\alpha_i} f_{in}[t_k - (N_1 - 1 - n)h] \right] = b u(t_k). \quad (33)$$

By rearranging (33) we obtain:

$$\sum_{i=1}^N a_i A_i(t_k) + b u(t_k) = y(t_k) \quad (34)$$

where

$$A_i(t_k) = -\frac{1}{h^{\alpha_i}} \left[\sum_{j=0}^{N_1} C_j^{\alpha_i} y(t_{k-j}) + \sum_{n=0}^{N_3-1} C_n^{\alpha_i} f_{in}[t_k - (N_1 - 1 - n)h] \right] \quad (35)$$

Accordingly, the reformulated discrete initialized discretized estimation problem (IDEP) is given in the following proposition.

Proposition 1. *For a given small enough sampling time h , the estimation problem (EP) can be reformulated in the discrete space as follows:*

$$F(\alpha; N_3) \cdot p = R, \quad (36)$$

where p is the vector of unknown parameters and $R \in \mathbb{R}^{K \times 1}$ such that $K = N_1 - N_3$, the number of samples within $[t_{in}, T]$, $R_k = y(t_k)$, $k = 1, 2, \dots, K$.

The function $F(\alpha; N_3) \in \mathbb{R}^{K \times (N+1)}$ that is a non-linear function with respect to the fractional differentiation orders and the length of the initialization memory is given as follows: for $\forall k = 1 : K$

$$F_{ki}(\alpha_i; N_3) = \begin{cases} A_i(t_k) = -\frac{1}{h^{\alpha_i}} \left[\sum_{j=0}^{N_1} C_j^{\alpha_i} y(t_{k-j}) + \sum_{n=0}^{N_3-1} C_n^{\alpha_i} f_{in}[t_k - (N_1 - 1 - n)h] \right], \\ \forall i = 1 : N \\ u(t_k), \text{ for } i = N + 1, \end{cases} \quad (37)$$

Remark 2. *It is worth noting that the reformulated problem (36) is expressed as a linear combination of nonlinear functions. The unknown variables in the objective function based on in (36), can be separated into two disjoint sets: linear variables, p , and nonlinear variables, $(\alpha; N_3)$. This class of problems is known as the separable nonlinear least squares problem [20].*

5 Estimation algorithm

This section introduces the main two steps of the proposed method to solve (EP). The first step designs a time-varying history function to initialize the output signal of the FOS (27). The second step is an iterative hybrid approach to solve the estimation problem of the unknown parameters and fractional differentiation orders, (36). This step contains two stages. The first stage solves the

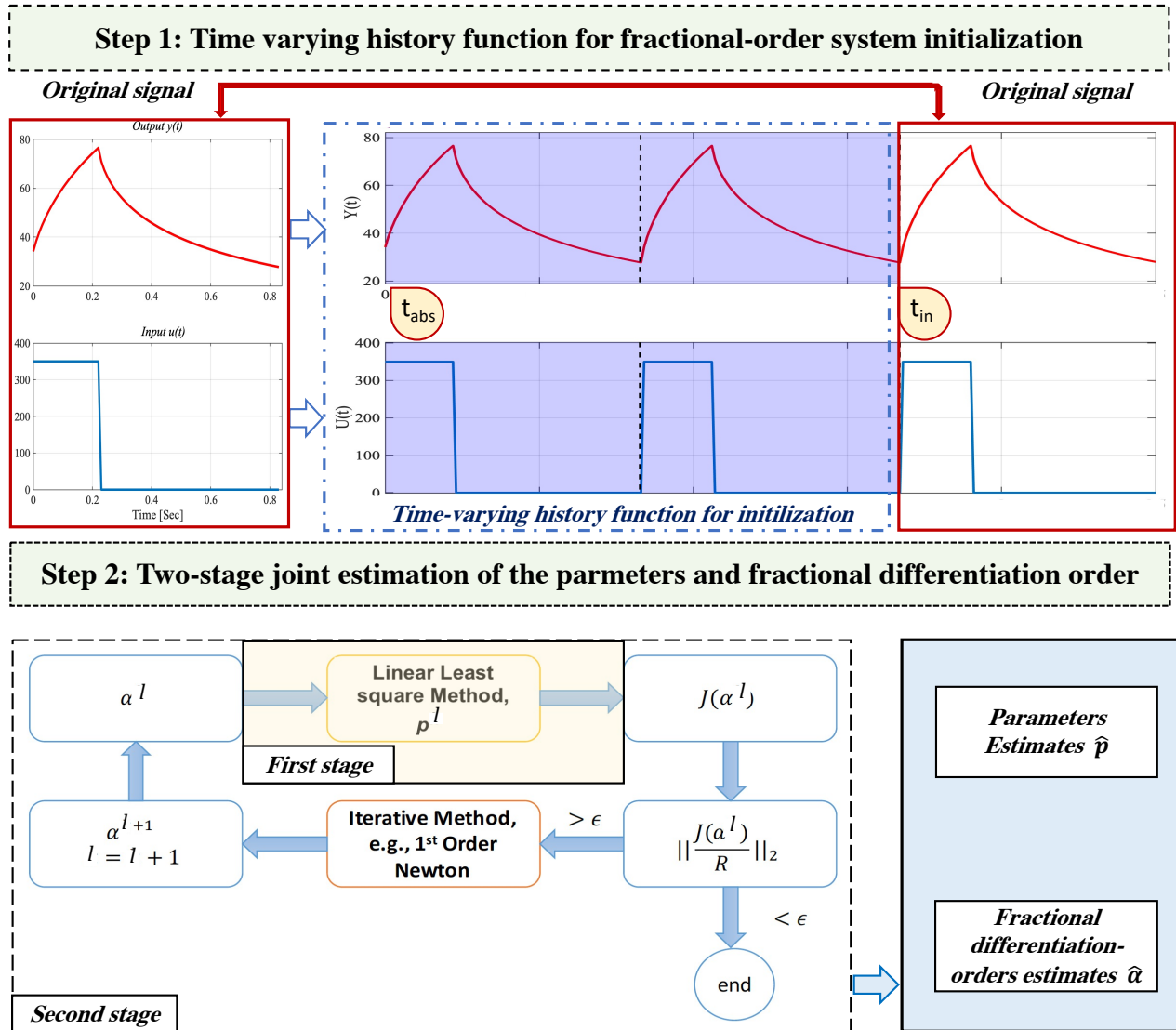


Figure 4: A flowchart showing the two main steps of initialized estimation algorithm for parameters and fractional differentiation orders of fractional-order systems.

parameters' estimation problem at each iteration using a linear least square method by solving a linear system of equations; the second stage solves a nonlinear system of equations using Newton's method to find estimates for the fractional differentiation orders. The main steps of the proposed

method which are explained in the following are depicted in Figure 4.

5.1 Step 1: Design of the time-varying history function

The key hypothesis in step 1 is to propose an initialization function, $f_{in}(t)$, in the estimation process of the unknown parameters and fractional differentiation orders. The choice of $f_{in}(t)$ depends on the available measured output $y(t)$ where duplicates of $y(t)$ is considered. This choice reduces the infinite-dimensional space of possible initialization functions into a finite parametric space where the remaining degree of freedom is the number of output cycles to be duplicated. A schematic picture of the designed initialization framework (function) is depicted in Figure 4, Step 1.

5.2 Step 2: Two-stage Estimation Algorithm for Parameters and Fractional Differentiation Order

Let the fractional derivatives of the output signal, $y(t)$, be initialized with a time-varying function $f_{in}(t)$ as designed in the previous step. In this study, we suppose that N_3 is known. Accordingly, in this situation the set of parameters p enters linearly while the set of parameters α non-linearly in the following predictor:

$$\hat{y}(t | p, \alpha) = p^{tr} F^{tr}(t, \alpha; N_3). \quad (38)$$

The identification criterion then becomes

$$V_K(p, \alpha) = \sum_{k=1}^K |y(t_k) - p^{tr} F^{tr}(t_k, \alpha; N_3)|^2 = |R - F(\alpha; N_3)p|^2, \quad (39)$$

where we introduced matrix notation, analogously to (36). Then, for a given α , this criterion is the least square criterion and minimized w.r.t. p by

$$\hat{p} = [F^{tr}(\alpha; N_3)F(\alpha; N_3)]^{-1} F^{tr}(\alpha; N_3) R \quad (40)$$

By inserting (40) into the identification criterion (39) the non-linear problem with respect to α can be defined as:

$$\min_{\alpha} \|R - P(\alpha)R\|^2 = \min_{\alpha} \|[I_{K \times K} - P(\alpha)]R\|^2 := \min_{\alpha} \|J(\alpha; N_3)\|^2 \quad (41)$$

where

$$J(\alpha; N_3) = [I_{K \times K} - P(\alpha)]R \quad (42)$$

with $I_{K \times K}$ being the identity matrix of dimension K and $P(\alpha)$ is defined as:

$$P(\alpha) = F(\alpha; N_3) \left[F^{tr}(\alpha; N_3) F(\alpha; N_3) \right]^{-1} F^{tr}(\alpha; N_3) \quad (43)$$

Remark 3. *The estimate \hat{p} is obtained by inserting the minimizing α into (42). The matrix P is a projection matrix: $P^2 = P$. The described method is called separable least squares since the least-square part has been separated out, and the problem is reduced to a minimization problem of lower dimension.*

An estimate $\hat{\alpha}^l$ of the vector of fractional differentiation orders are computed iteratively by solving the nonlinear problem:

$$J(\alpha; N_3) = 0 \quad (44)$$

with $J \in \mathbb{R}^{K \times 1}$, which is defined in Eq. (42), using the following Newton update law:

$$\hat{\alpha}^{l+1} = \hat{\alpha}^l - [J'(\hat{\alpha}^l; N_3)]^{-1} J(\hat{\alpha}^l; N_3), \quad (45)$$

where $J'(\alpha; N_3) \in \mathbb{R}^{K \times N}$ is the Jacobian matrix of the nonlinear function J .

Proof. The system of equations (36) is solved in two stages. While in the first step we use the linear least square method to estimate the parameters, in the second step we use *Newton* iterative method to estimate the fractional differentiation orders.

First stage: From (36) we have

$$F(\alpha^l; N_3) \cdot p = R, \quad (46)$$

For any given α , we denote \hat{p} the solution of (46) for the unknown vector of parameters p . Thus, for $\alpha = \hat{\alpha}^l$ the system of equations(46) can be written as in (40).

Second stage: From (36) and the first stage we have

$$F(\alpha; N_3) \cdot \hat{p} = R, \quad (47)$$

where $F(\alpha; N_3)$ and R are introduced in (37). We propose to use the iterative first-order Newton method to solve(47), with a solution at iteration l denoted $\hat{\alpha}^l$. The Newton update law is given in (45). At each iteration, (44) follow directly from (47).

The Jacobian matrix ($J'(\alpha)$) needs to be evaluated at each iteration l . Thus, we first substitute α by α^l , and then we use it in the updated law (45). □

The main steps of the proposed method are given in Algorithm 1.

6 Convergence of the algorithm

6.1 Characterization of the Jacobian matrix

In this part, we show the analytical derivation of the Jacobian matrix $J'(\alpha)$. The following lemmas are needed in the derivation of the Jacobian matrix and the convergence of the proposed algorithm.

Lemma 1. [21], *Let $M \in R^{K \times N}$. $M^{tr}M$ is called the Gram matrix of M . The Moore-Penrose inverse of M is M^+ and we have:*

$$M^+ = (M^{tr}M)^+ M^{tr} = M^{tr}(M M^{tr})^+. \quad (48)$$

Algorithm 1 Proposed two-stage estimation method

- 1: initialize $l = 0$, give an initial guess to α^l ,
 - 2: compute \hat{p} using equation (40) ,
 - 3: compute $J(\alpha^l)$ using equations (42),
 - 4: **if** $\| \frac{J(\alpha^l)}{R} \| \prec \epsilon$ then²
 - 5: stop
 - 6: **else**
 - 7: update α^l using equations,
 - 8: update the number of iterations $l = l + 1$,
 - 9: return to step 2
 - 10: **end if**
-

Lemma 2. *Let $M(\alpha)$ be a defined on an interval I whose values are nonzero $n \times n$ matrices, differentiable at α^* . Then the function M^+ is differentiable at α^* if and only if $\text{rank}(M(\alpha))$ is constant in some interval $|\alpha - \alpha^*| < \delta$. The derivative of the $\frac{\partial M^+}{\partial \alpha}(\alpha^*)$ is given by:*

$$\frac{\partial M^+}{\partial \alpha} = -M^+ \left(\frac{\partial M}{\partial \alpha} \right) M^+ + M^+ (M^+)^{tr} \left(\frac{\partial M^{tr}}{\partial \alpha} \right) e + e \left(\frac{\partial M^{tr}}{\partial \alpha} \right) (M^+)^{tr} M^+, \quad (49)$$

where $e = (I - MM^+)$ and $M, M^{tr}, M^+, \frac{\partial M}{\partial \alpha}$ stand for $M(\alpha^*), M^{tr}(\alpha^*), M^+(\alpha^*), \frac{\partial M}{\partial \alpha}(\alpha^*)$ respectively.

Based on the formulation of $J(\alpha; N_3)$ in (42) and (43) the elements of the Jacobian matrix $J'(\alpha; N_3)$ can be computed as: $\forall i = 1 : K$ and, $j = 1 : N$:

$$J'_{ij} = \frac{\partial J_i}{\partial \alpha_j} = \sum_{l=1}^K \frac{\partial}{\partial \alpha_j} P_{il}(\alpha) R_l. \quad (50)$$

Such that:

$$P(\alpha) = F(\alpha) \overbrace{\left[\underbrace{F^{tr}(\alpha)F(\alpha)}_{\text{Gram matrix}} \right]^{-1}}^{F^+} F^{tr}(\alpha). \quad (51)$$

The matrix $F(\alpha)$ can be expressed as:

$$F(\alpha) = \begin{pmatrix} F_{11}(\alpha) & F_{12}(\alpha) & F_{13}(\alpha) & \dots & F_{1(N+1)}(\alpha) \\ F_{21}(\alpha) & F_{22}(\alpha) & F_{23}(\alpha) & \dots & F_{2(N+1)}(\alpha) \\ F_{31}(\alpha) & F_{32}(\alpha) & F_{33}(\alpha) & \dots & F_{3(N+1)}(\alpha) \\ \cdot & \cdot & \cdot & \dots & \cdot \\ \cdot & \cdot & \cdot & \dots & \cdot \\ \cdot & \cdot & \cdot & \dots & \cdot \\ F_{K1}(\alpha) & F_{K2}(\alpha) & F_{K3}(\alpha) & \dots & F_{K(N+1)}(\alpha) \end{pmatrix} \quad (52)$$

Based on **Lemma. 1**, we note:

$$B = F^+ = \left[F^{tr}(\alpha)F(\alpha) \right]^{-1} F^{tr}(\alpha) = \left[F^{tr}(\alpha)F(\alpha) \right]^+ F^{tr}(\alpha), \quad (53)$$

is the *Moore-Penrose* inverse matrix. Accordingly, (51) can be written as:

$$P(\alpha) = F(\alpha) F^+(\alpha) = F(\alpha) B(\alpha), \quad (54)$$

where $B(\alpha)$ is defined as:

$$B(\alpha) = F^+(\alpha) = \begin{pmatrix} B_{11}(\alpha) & B_{12}(\alpha) & B_{13}(\alpha) & \dots & B_{1K}(\alpha) \\ B_{21}(\alpha) & B_{22}(\alpha) & B_{23}(\alpha) & \dots & B_{2K}(\alpha) \\ B_{31}(\alpha) & B_{32}(\alpha) & B_{33}(\alpha) & \dots & B_{3K}(\alpha) \\ \cdot & \cdot & \cdot & \dots & \cdot \\ \cdot & \cdot & \cdot & \dots & \cdot \\ \cdot & \cdot & \cdot & \dots & \cdot \\ B_{(N+1)1}(\alpha) & B_{(N+1)2}(\alpha) & B_{(N+1)3}(\alpha) & \dots & B_{(N+1)K}(\alpha) \end{pmatrix} \quad (55)$$

The elements of the matrix $P(\alpha)$ are defined as follows:

$\forall i = 1 : K$ and $l = 1 : K$

$$P_{il}(\alpha) = \sum_{m=1}^{N+1} F_{im}(\alpha) B_{ml}(\alpha). \quad (56)$$

and its derivative with respect to the fractional differentiation order α can be evaluated as:

$$\frac{\partial P_{il}(\alpha)}{\partial \alpha_j} = \sum_{m=1}^{N+1} F_{im}(\alpha) \frac{\partial B_{ml}(\alpha)}{\partial \alpha_j} + \sum_{m=1}^{N+1} \frac{\partial F_{im}(\alpha)}{\partial \alpha_j} B_{ml}(\alpha) \quad (57)$$

where $\frac{\partial B_{ml}(\alpha)}{\partial \alpha_j}$ are the element of the derivative of Moore-Penrose inverse matrix which can be

computed using **Lemma. 2**.

$\frac{\partial F_{im}(\alpha)}{\partial \alpha_j}$ is derived based on the formulation of (37) as:

$$\frac{\partial F_{im}}{\partial \alpha_j} = \begin{cases} -\frac{\ln(h)}{h^{\alpha_m}} \left[\sum_{l=1}^{N_1} C_l^{\alpha_m} y(t_{i-l}) + \sum_{n=1}^{N_3-1} C_n^{\alpha_m} f_{in} [t_i - (N_1 - 1 - n)h] \right] - \\ \frac{1}{h^{\alpha_m}} \left[\sum_{l=0}^{N_1} \frac{\partial C_l^{\alpha_m}}{\partial \alpha_m} y(t_{i-l}) + \sum_{n=0}^{N_3-1} \frac{\partial C_n^{\alpha_m}}{\partial \alpha_m} f_{in} [t_i - (N_1 - 1 - n)h] \right] & j = m \\ 0 & j \neq m \end{cases} \quad (58)$$

where $\ln(\cdot)$ is logarithmic function and the partial derivative of the binomial coefficients with respect to α_j is computed iteratively as follows:

$$\frac{\partial C_n^{\alpha_j}}{\partial \alpha_j} = \begin{cases} 0 & n = 0 \\ \frac{-1}{n} C_{n-1}^{\alpha_j} + \left(1 - \frac{1 + \alpha_j}{n}\right) \frac{\partial C_{n-1}^{\alpha_j}}{\partial \alpha_j} & n \geq 1 \end{cases} \quad (59)$$

Substituting (57) in (50) the element of the Jacobian matrix, $J'(\alpha)$ can be computed using the following expression:

$$J'_{ij}(\alpha) = \sum_{l=1}^K \sum_{m=1}^{N+1} F_{im}(\alpha) \frac{\partial B_{ml}(\alpha)}{\partial \alpha_j} + \sum_{l=1}^K \frac{\partial F_{ij}}{\partial \alpha_j} B_{jl} \quad (60)$$

The matrix J' can be expressed as:

$$J'(\alpha) = \begin{pmatrix} \frac{\partial J_1}{\partial \alpha_1} & \frac{\partial J_1}{\partial \alpha_2} & \frac{\partial J_1}{\partial \alpha_3} & \cdots & \frac{\partial J_1}{\partial \alpha_{N+1}} \\ \cdot & \cdot & \cdot & \cdots & \cdot \\ \cdot & \cdot & \cdot & \cdots & \cdot \\ \cdot & \cdot & \cdot & \cdots & \cdot \\ \frac{\partial J_K}{\partial \alpha_1} & \frac{\partial J_K}{\partial \alpha_2} & \frac{\partial J_K}{\partial \alpha_3} & \cdots & \frac{\partial J_K}{\partial \alpha_{N+1}} \end{pmatrix} \quad (61)$$

6.2 Proof of convergence

The iterative character of the above algorithm results from the Newton method which is used to estimate the fractional differentiation order, α . The vector of parameters p is estimated by solving the least square problem. However, we note that this estimate depends on the vector of fractional orders α .

Thus, we use a standard convergence result of Newton's method to provide sufficient conditions to ensure the local convergence of the proposed two-stage algorithm. Such a result can be found in Chapter 5 of [22]. We also make use of two results on Lipschitz functions stating that the product and quotient (denominator not zero) of two bounded Lipschitz functions are Lipschitz. The following assumptions are needed to prove the convergence result stated in Theorem 1.

Assumption 1. *The input $u(t)$, output $y(t)$ and the initialization function $f_{in}(t)$ are bounded functions in $[0, T]$.*

Assumption 2. *A solution α^* to the system $J(\alpha) = 0$ exists.*

Assumption 3. *The Jacobian matrix $J'(\alpha^*)$ is nonsingular.*

Theorem 1. *Assume that Assumptions 1–3 hold. Then, the proposed proposed two-stage algorithm converges q -quadratically.*

Proof. Based on Theorem 5.1.2, page 71 in [22], and given Assumptions 2 and 3, it remains to prove that the Jacobian matrix is Lipschitz continuous for $\alpha \in \wp = (n_{i-1}, n_i)$ ³ in order to conclude about the convergence of the proposed two-stage algorithm.

The entries of the Jacobian matrix are given by (60) where the terms F_{im} , $\frac{\partial F_{im}(\alpha)}{\partial \alpha_j}$, B_{jl} and $\frac{\partial B_{ml}(\alpha_j)}{\partial \alpha_j}$ are characterized in (37), (58), (53) and Lemma 2, respectively.

The norm 1 of the term $J'(\alpha^1) - J'(\alpha^2)$ is given as follows:

$$\begin{aligned}
\| J'(\alpha^1) - J'(\alpha^2) \|_1 &= \max_{1 \leq j \leq N} \sum_{i=1}^K | J'_{ij}(\alpha^1) - J'_{ij}(\alpha^2) | \\
&= \max_j \sum_{i=1}^K \left| \left(\sum_{l=1}^K \sum_{m=1}^{N+1} F_{im}(\alpha^1) \frac{\partial B_{ml}}{\partial \alpha_j}(\alpha^1) + \sum_{l=1}^K \frac{\partial F_{ij}}{\partial \alpha_j} B_{jl} \right) \right. \\
&\quad \left. - \sum_{l=1}^K \sum_{m=1}^{N+1} F_{im}(\alpha^2) \frac{\partial B_{ml}}{\partial \alpha_j}(\alpha^2) + \sum_{l=1}^K \frac{\partial F_{ij}}{\partial \alpha_j}(\alpha^2) B_{jl} \right| \tag{62} \\
&= \sum_{i=1}^K \left| \sum_{l=1}^K \sum_{m=1}^{N+1} \left\{ F_{im}(\alpha^1) \frac{\partial B_{ml}}{\partial \alpha_{j^*}}(\alpha^1) - F_{im}(\alpha^2) \frac{\partial B_{ml}}{\partial \alpha_{j^*}}(\alpha^2) \right\} + \right. \\
&\quad \left. \left(\sum_{l=1}^K \left\{ \frac{\partial F_{ij^*}}{\partial \alpha_{j^*}}(\alpha^1) B_{j^*l}(\alpha^1) - \frac{\partial F_{ij^*}}{\partial \alpha_{j^*}}(\alpha^2) B_{j^*l}(\alpha^2) \right\} \right) \right|
\end{aligned}$$

where j^* is the column index corresponding to the maximum of the sum of the row components.

³ $\wp = \prod_{i=1}^N \wp_i = \{(a_1, a_2, \dots, a_N) | \forall i = 1, 2, \dots, N, a_i \in \wp_i\}$ is the generalized Cartesian product of N sets $\wp_1, \wp_2 \dots \wp_N$.

Then, using the triangle inequality, (62) can be written as follows:

$$\begin{aligned} & \| J'(\alpha^1) - J'(\alpha^2) \|_1 \leq \\ & \sum_{i=1}^K \sum_{l=1}^K \sum_{m=1}^{N+1} \left| F_{im}(\alpha^1) \frac{\partial B_{ml}}{\partial \alpha_{j^*}}(\alpha^1) - F_{im}(\alpha^2) \frac{\partial B_{ml}}{\partial \alpha_{j^*}}(\alpha^2) \right| \\ & + \sum_{i=1}^K \sum_{l=1}^K \left| \frac{\partial F_{ij^*}}{\partial \alpha_{j^*}}(\alpha^1) B_{j^*l}(\alpha^1) - \frac{\partial F_{ij^*}}{\partial \alpha_{j^*}}(\alpha^2) B_{j^*l}(\alpha^2) \right| \end{aligned} \quad (63)$$

Given the right hand side of inequality (63) and using properties on Lipschitz functions, if $F_{im}(\alpha)$ and $\frac{\partial F_{ij}}{\partial \alpha_j}(\alpha)$ are Lipschitz continuous and $B_{jl}(\alpha)$ and $\frac{\partial B_{ml}}{\partial \alpha_j}(\alpha)$ are bounded then we can conclude about the Lipschitz continuity of $J'(\alpha)$.

Given that C_l^α and $\frac{\partial C_l^\alpha}{\partial \alpha}$ is high-order polynomial of α then they are Lipschitz continuous. In addition, $\left(\frac{1}{h^\alpha}\right)$ is bounded on bounded local interval of α . Accordingly, and taking into account *Assumption 1* we can insure the Lipschitz continuity of $F_{im}(\alpha)$ and $\frac{\partial F_{ij}}{\partial \alpha_j}(\alpha)$.

With respect to the boundedness of $B_{jl}(\alpha)$ and $\frac{\partial B_{ml}}{\partial \alpha_j}(\alpha)$, based on the proof in [] that confirm that if $F(\alpha)$ has a constant rank for $\alpha^* - \delta < \alpha \leq \alpha^* + \delta$ then its Moore-Penrose inverse B is differentiable at α^* and its derivative is computed using *Lemma 2*. Accordingly the of B_{jl} and its derivative follows from this condition.

7 Numerical Results

The performance of the proposed method is illustrated through different numerical examples. Furthermore, potential applications of the algorithm are presented, which consists of estimating parameters and fractional differentiation orders of 1) fractional-order two-element arterial Windkessel (*F-WK2*)

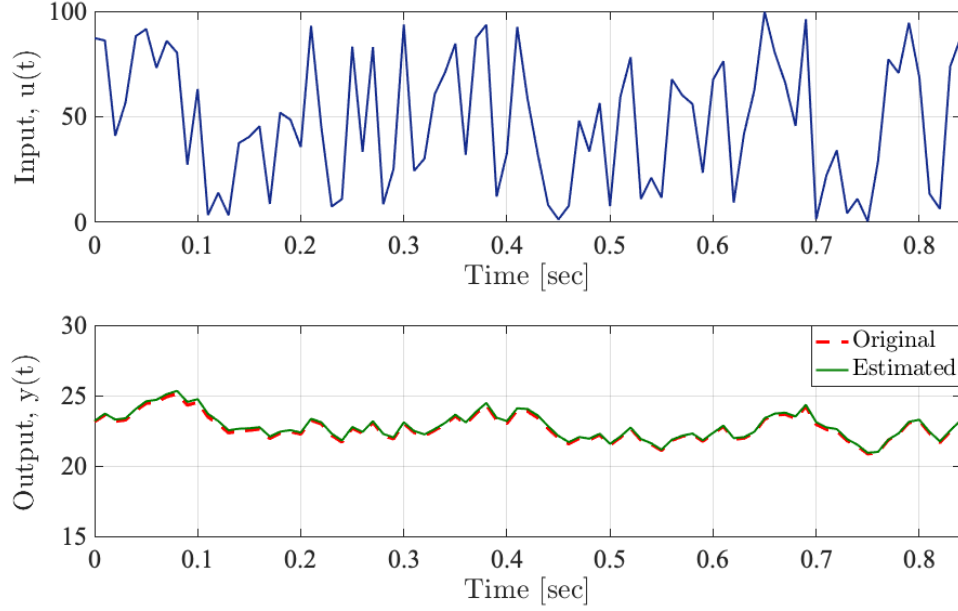


Figure 5: Estimated output signal along with the real one using random input signal. Here we use $N_0 = 15$ and $N_C = 10$. The sampling rate $h = 0.01$ has been used in this simulation.

model and 2) fractional-order neurovascular model. In the following analysis of the results, we consider the percent relative error $Re(\%)$ as a measure of estimation accuracy. In the case of parameter p estimation, the $Re_p(\%)$ is defined as:

$$Re_p = \frac{|\hat{p} - p|}{|p|} \times 100, \quad (64)$$

where \hat{p} denotes the estimate of p . In the case of signal estimation y , the $Re_y(\%)$ is defined as:

$$Re_y = \frac{\|\hat{y} - y\|_2}{\|y\|_2} \times 100, \quad (65)$$

where \hat{y} denotes the estimate of the real measurement y .

7.1 Example 1

We consider the following fractional-order system:

$$y(t) + a_1 {}_{t_{in}}D_t^\alpha y(t) = b u(t) \quad t \in [0, 0.84] \quad (66)$$

Here we consider two numerical cases based on the nature of the input signal $u(t)$, namely: Random input signal and periodic pulse train input signal.

7.1.1 Random input signal

In this example, we consider the system described in (66) with a random input signal whose amplitude varies between 0 and 100. The parameters and fractional differentiation order are $a_1 = 1$, $b = 0.5$ and $\alpha = 0.7$. A sensitivity analysis of the proposed algorithm with respect to the length of the time-varying history function-based output fractional-order derivative initialization, N_3 , and the length of the original signal was performed. In addition, a sensitivity analysis with respect to the initial guess of Newton's method (the initial guess of the fractional differentiation order α^0) is performed. We note $N_C = N_3/L$ and $N_0 = K/L$ where L corresponds to the length of the original output signal and K is the total number of samples used for estimation, following the previous notations, it is defined as $K = N_1 - N_3$.

Figure 5 shows the input signal and the estimated output signal along with the original one for $N_0 = 15$ and $N_C = 10$. In this case, the relative errors of the parameters estimate a_1 and b were 11.77% and 0.13% respectively, whereas, for the fractional differentiation order estimate, it was 3.93% and the reconstructed output around 1.22%. It is clear from these results that we have a good estimation performance for the output signal. Although the estimation error of the parameters and the fractional differentiation order is not the best, we still have a good reconstruction of the output. The reason is that in this case, we cannot insure the global identifiability of the system (66).

Figure 6 shows a contour plot of the relative errors (%) with respect to the number of cycles based time-varying history function, N_C , and the number of original cycles based for estimation, N_0 for the parameters, fractional differentiation order and the reconstructed output. Overall, from these

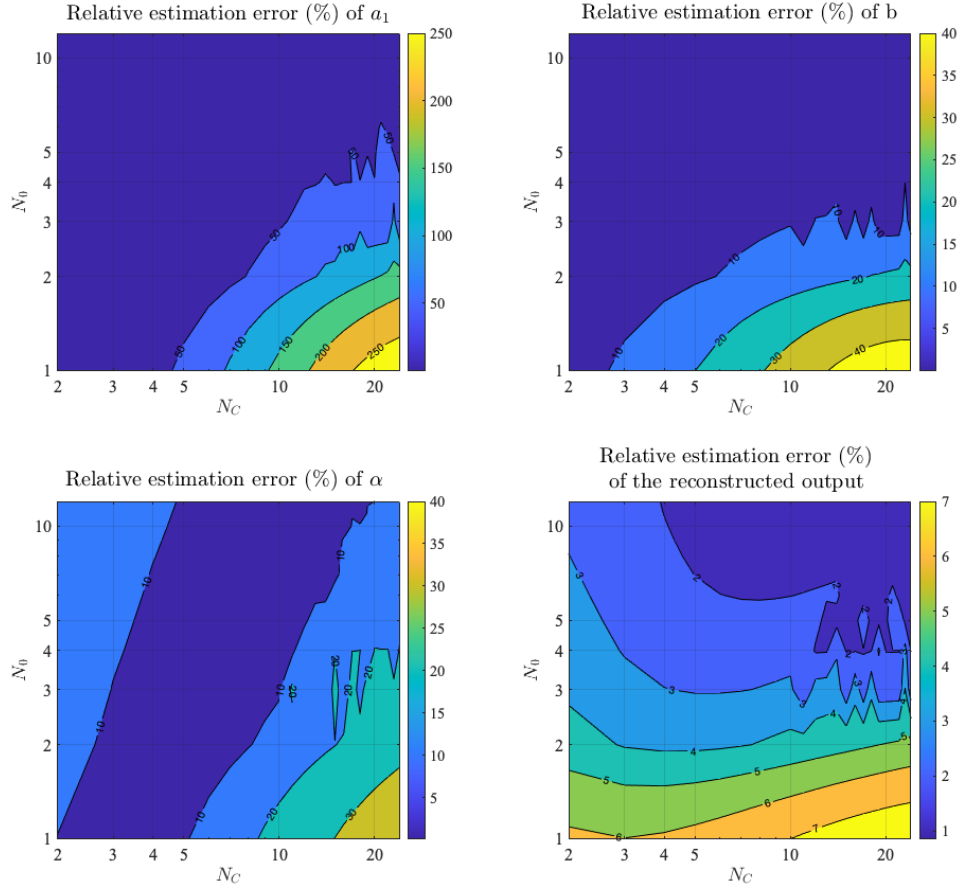


Figure 6: Contour plot of the relative error (%) with respect to the number of cycles based time-varying history function, N_C and the number of original cycles based for estimation, N_0 for: parameter (a_1), parameter (b), the fractional differentiation order (α) and the reconstructed output signal (y). The sampling rate $h = 0.01$ has been used in this simulation.

subplots it is clear that increasing both N_C and N_0 leads to a decrease in the relative error and so better estimation for the parameters, fractional differentiation order, and the reconstructed output. For a fixed N_C we noticed that as N_0 increases the relative error decreases.

With regards to the unknown parameters and α , there are optimal values of (N_C^*, N_0^*) that lead to the minimum error. Any combination larger than (N_C^*, N_0^*) might lead to a small increase in the error. With respect to the output relative error, we noticed that increasing more N_0 leads to better

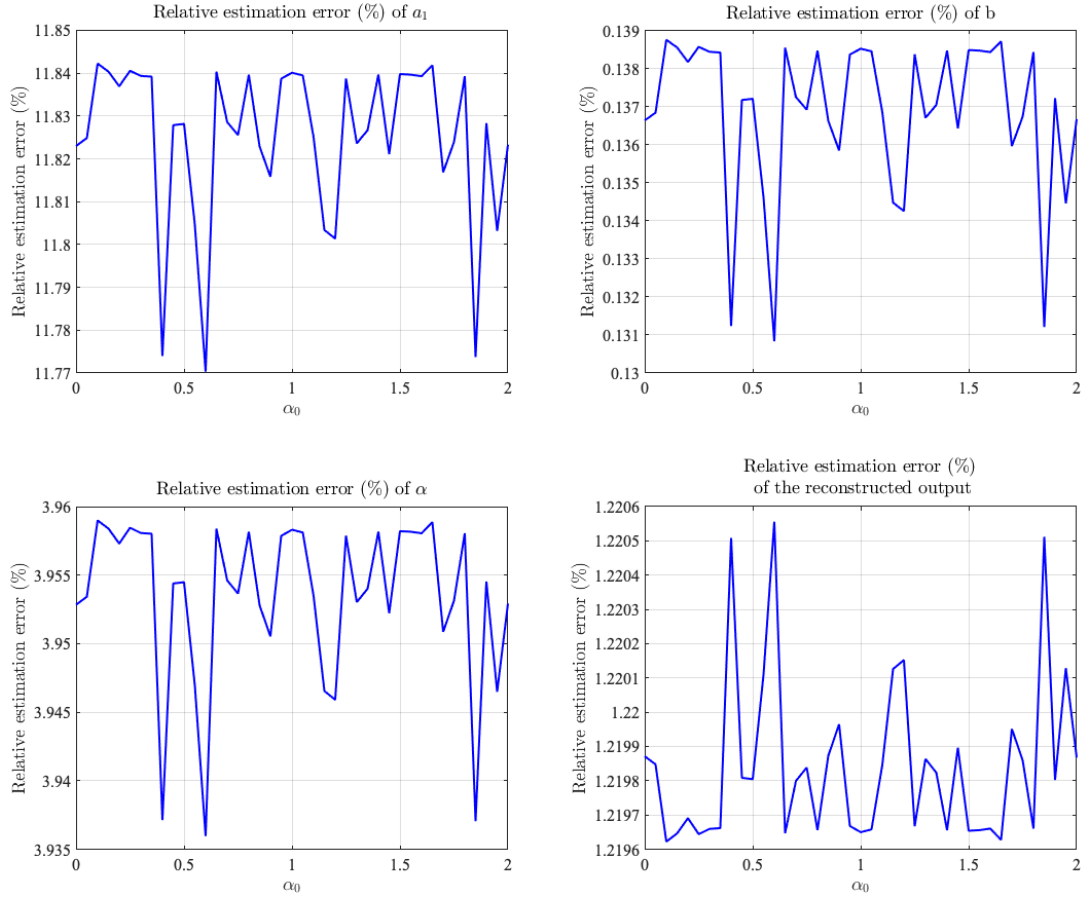


Figure 7: Relative error (%) with respect to the initial guess of the fractional differentiation order α_0 for: parameter (a_1), parameter (b), the fractional differentiation order (α) and the reconstructed output signal (y). The sampling rate $h = 0.01$ has been used in this simulation.

performances. For small values of $N_0 = 1, 2, \dots, 5$ it is clear that there is the optimal combination (N_C^*, N_0^*) that leads to the best performance.

Figure 7 summarizes the results of the relative errors of the estimated unknowns when the initial guess of Newton's method is varying. In this simulation we varied α^0 from 0.05 to 2 with a step of 0.05. It is clear that the proposed algorithm is not very sensitive to initial guesses in this case.

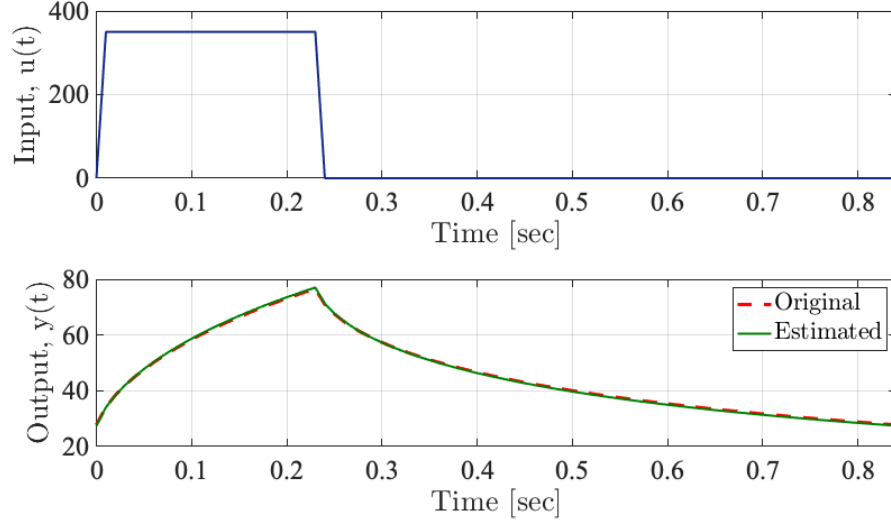


Figure 8: Estimated output signal along with the real one using random input signal. Here we use $N_0 = 15$ and $N_C = 10$. The sampling rate $h = 0.01$ has been used in this simulation.

7.1.2 Periodic pulse train input signal

In this example we consider the system described in (66) where the parameters and fractional differentiation order are $a_1 = 1$, $b = 0.5$ and $\alpha = 0.7$. The input $u(t)$ is taken as a periodic pulse train of duration $T = 0.84$ [s], an amplitude $A = 350$ and a duty cycle ($d_C = 0.27$). The time step used in this example is $h = 0.01$. Similar to the previous example, a sensitivity analysis of the proposed algorithm with respect to the length of the time-varying history function-based output fractional-order derivative initialization, the length of the original signal and the initial guess of Newton's method is performed. Figure 8 summarizes the reconstruction results of the output of the fractional-order system (66) using a periodic pulse train signal as an output. In this simulation we used ($N_0 = 15; N_C = 10$). The relative errors of this reconstruction is 1.19%, for the unknown parameter a_1 is 2.42% and b is 1.56% and the fractional-differentiation order is 0.35%.

In figure 9, we summarize the results of the relative errors of the estimated unknowns and the recon-

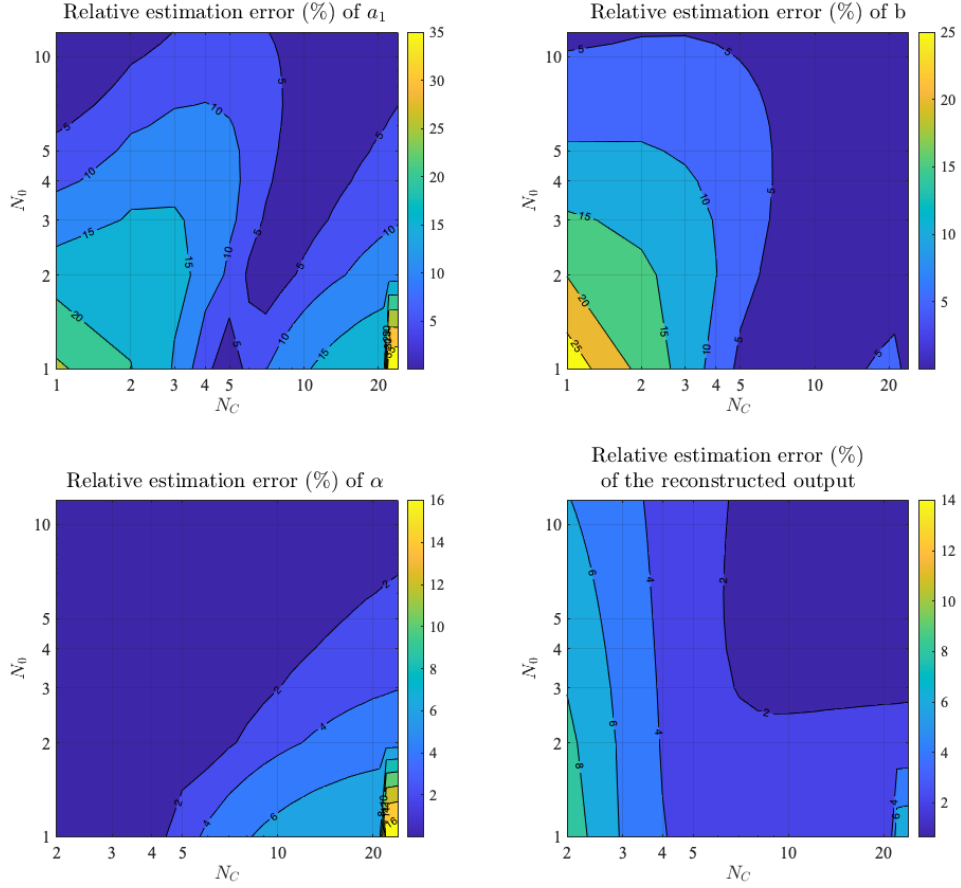


Figure 9: Contour plot of the relative error (%) with respect to the number of cycles based time-varying history function, N_C and the number of original cycles based for estimation, N_0 for: parameter (a_1), parameter (b), the fractional differentiation order (α) and the reconstructed output signal (y). The sampling rate $h = 0.01$ has been used in this simulation.

structed output for a different combination of $(N_0; N_C)$.

Figure 10 summarizes the results of the relative errors of the estimated unknowns when the initial guess of the fractional differentiation order, α^0 , is varying from 0.4 to 1.25 with a step 0.05.

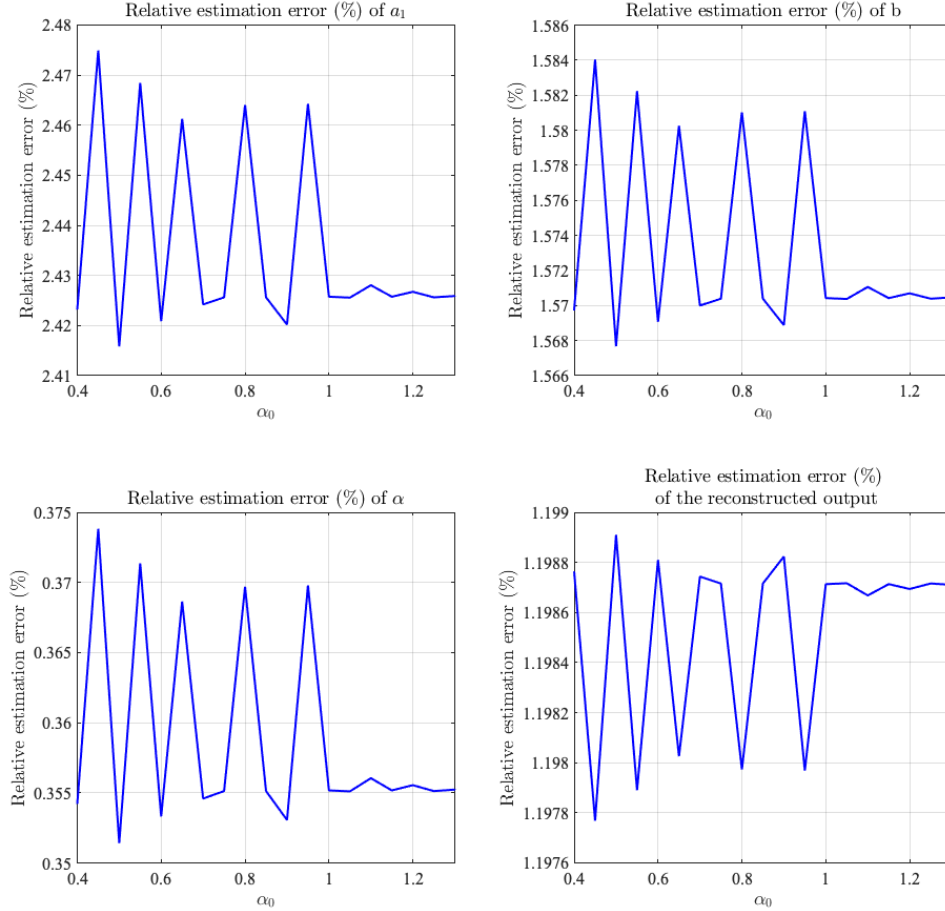


Figure 10: Relative error (%) with respect to the initial guess of the fractional differentiation order α_0 for: parameter (a_1), parameter (b), the fractional differentiation order (α) and the reconstructed output signal (y). The sampling rate $h = 0.01$ has been used in this simulation.

7.1.3 Joint estimation of the parameters and the fractional differentiation order of F-WK2

A potential application of the proposed algorithm is to estimate the hemodynamic parameters and the differentiation order of the fractional-order two-element arterial Windkessel (*F-WK2*). As shown in Fig. 11, *F-WK2* represents the heart as a current source that pumps blood into the arterial system, which is lumped into a single fractional-order capacitor and a single resistance [23, 24]. The fractional-order capacitor, characterized by two parameters (C_α, α), represents the apparent arterial compliance

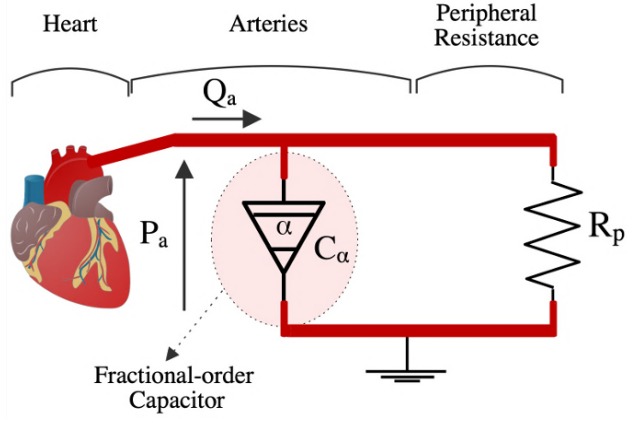


Figure 11: Fractional-order tow-element arterial Windkessel circuit model. C_α represents the arterial compliance and R_p represents the peripheral resistance.

by taking into account the viscoelastic properties of the vascular network via the fractional-order factor [25, 26]. The resistance R_p accounts for the total peripheral arterial resistance. The *F-WK2* system is given as follows:

$$P_a(t) + \tau_\alpha {}_{t_{in}}D_t^\alpha P_a(t) = R_p Q_a(t), \quad t \in [0, T_C] \quad (67)$$

where $\tau_\alpha = C_\alpha \cdot R_p$, $0 \leq \alpha \leq 1$ and T_C is the cardiac period. P_a corresponds to the aortic blood pressure, and Q_a denotes the aortic blood flow. To fully identify *F-WK2*, the hemodynamic parameters and the fractional differentiation order have to be estimated from measured flow and pressure waves from accessible arterial locations. This is also known as the hemodynamic inverse problem [27]. The proposed algorithm has been applied to an *in-silico* data generated from one-dimensional model [28]. Here, the aortic blood pressure is considered the output of the fractional-order system, while the aortic blood flow is considered the input. To initialize the fractional-order derivative of the output ($D_t^\alpha P_a(t)$), we used a certain number of cycles, N_C of the same output signal as a time-varying history function. We denote by N_0 the number of original cardiac cycles used for estimation. A sensitivity analysis of the applied algorithm with respect to N_C and (N_0) is performed.

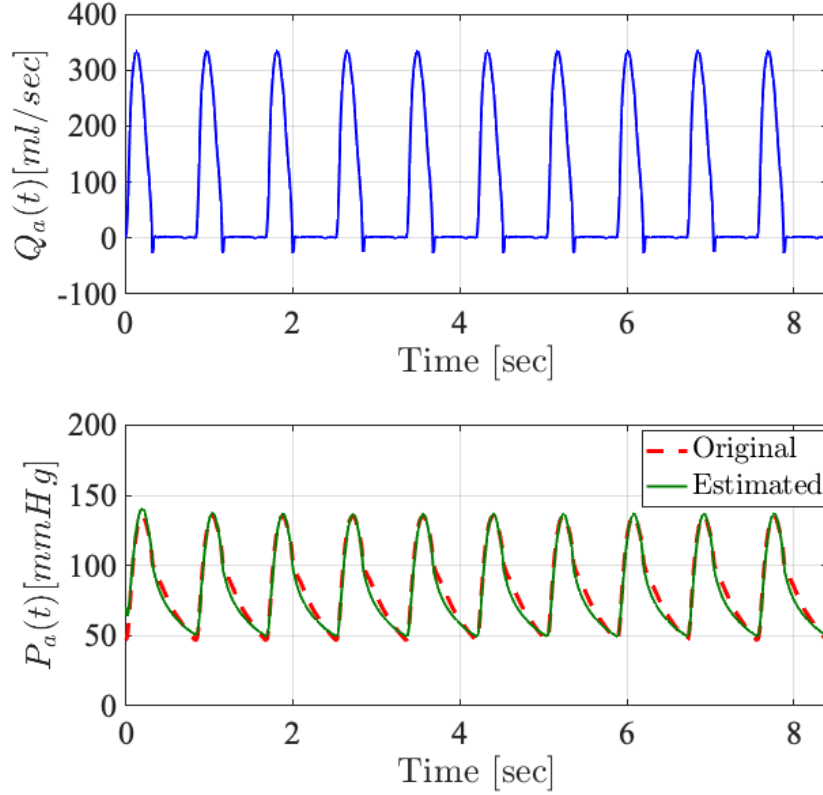


Figure 12: Estimated aortic blood pressure using $F-WK2$ along with the real one. Here we use $N_0 = 10$ and $N_C = 25$. The relative errors of the reconstructed output is 5.22%, $\tau_\alpha = 1.15$ and $R_p = 1.13$. The sampling rate $h = 0.01$ has been used in this simulation.

Fig. 12 summarizes the reconstruction results of 10 cardiac cycles of the aortic blood pressure using a real input and the estimated parameters and the fractional differentiation order. This reconstruction used 25 cycles to initialize the fractional-order derivative of the output and the relative error was around 5.22%. The estimate of the constant time is $\hat{\tau}_\alpha = 1.15$ and the peripheral resistance $\hat{R}_p = 1.13$. Figure 13 summarizes the sensitivity analysis of the relative error of the reconstructed aortic blood pressure (output of the system (67)) with respect N_C and N_0 . It is clear that as we increase N_C the relative error of the estimation decreases. Figure 14 summarizes the results of the relative errors of the estimated output the initial guess is varying from 0.35 to 1.2 with a step of 0.05

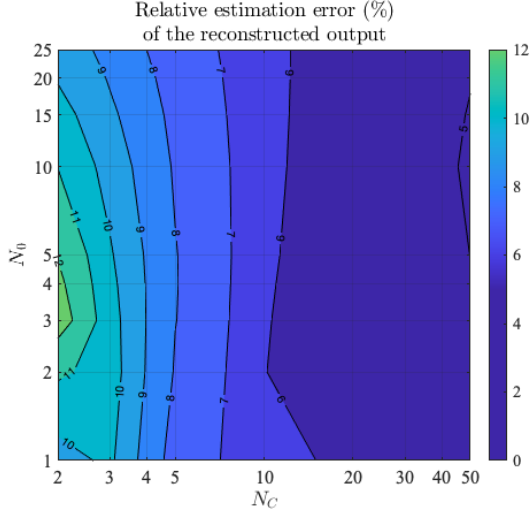


Figure 13: Relative estimation error vs. number of cycles based time-varying history function, N_C for one cycle output aortic blood pressure signal ($N_0 = 1$). The sampling rate $h = 0.01$ has been used in this simulation.

7.2 Example 2

We consider the following example:

$$y(t) + a_1 D_t^{\alpha_1} y(t) + a_2 D_t^{\alpha_2} y(t) = u(t), \quad t \in [0, 10] \quad (68)$$

where the parameters and fractional differentiation orders are $a_1 = 3$, $a_2 = 2$ and $\alpha_1 = 1.5$, $\alpha_2 = 0.5$.

Here we consider two numerical cases based on the nature of the input signal $u(t)$, namely: The *sinc* function as the input signal and the square input signal.

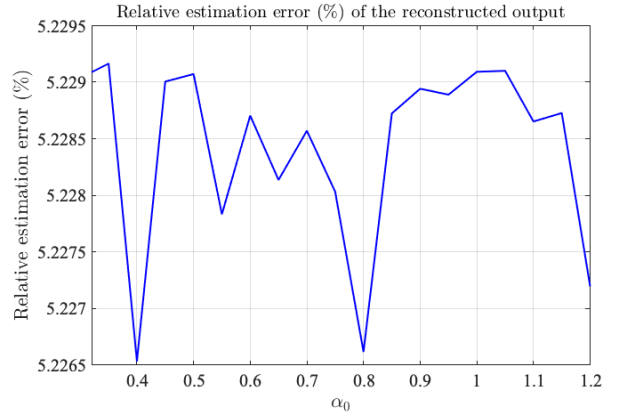


Figure 14: Relative error (%) with respect to the initial guess of the fractional differentiation order α_0 for the reconstructed output signal, the aortic blood pressure. The sampling rate $h = 0.01$ has been used in this simulation.

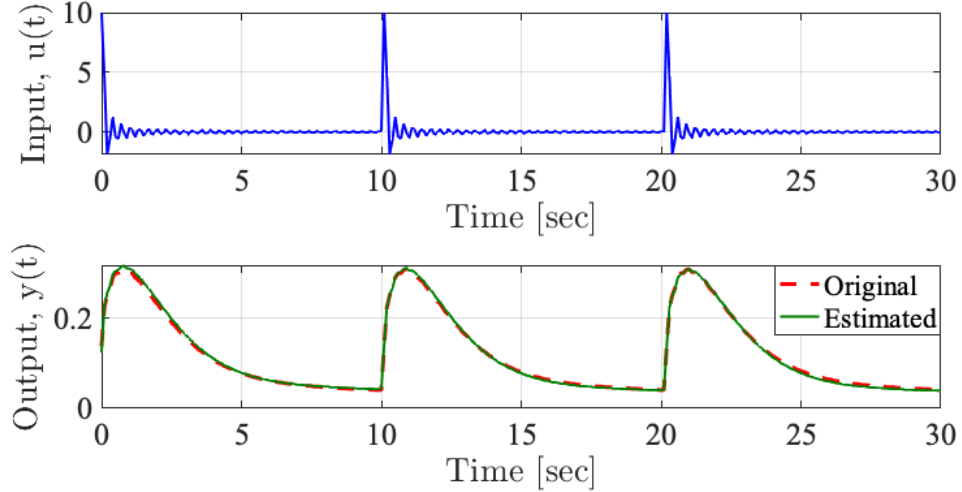


Figure 15: Estimated output signal along with the real one using random input signal. Here we use $N_0 = 3$ and $N_C = 10$. The sampling rate $h = 0.1$ has been used in this simulation.

7.2.1 *Sinc* function as an input signal

In this case, we consider the following profile for the input $u(t)$ in the system (68):

$$u(t) = 10\text{sinc}(2\pi t) \quad (69)$$

Figure 15 shows the reconstruction result of the estimated output using $N_C = 10$ and $N_0 = 3$. The relative errors of the unknown parameters $(a_1, a_2, \alpha_1, \alpha_2)$ are (1.45%, 1.60%, 0.33%, 3.61%) respectively and for the reconstructed output is 0.88%.

In figures 16, we summarize the results of the relative errors of the estimated unknowns parameters, fractional differentiation orders, and the reconstructed output for a different combination of $(N_0; N_C)$. From these results, it is clear that as the N_C increases the estimation accuracy increases. It is worth noting that for a small value of N_C increasing N_0 enhances the estimation accuracy.

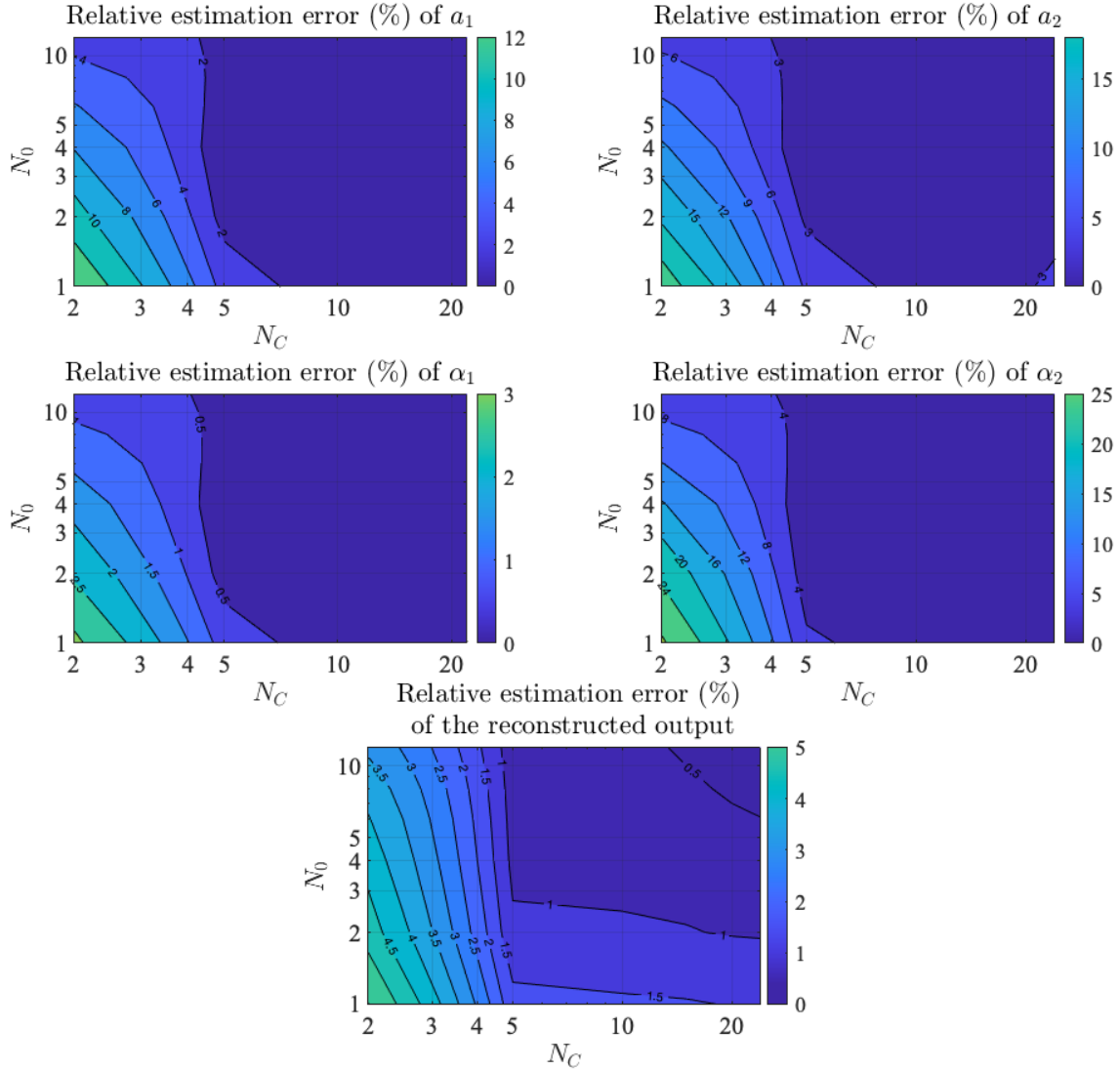


Figure 16: Contour plot of the percent relative error (%) with respect to N_C and N_0 for parameters, fractional differentiation orders and the reconstructed output. The sampling rate $h = 0.1$ has been used in this simulation.

7.2.2 Square input signal

In this example the input $u(t)$ of the fractional-order system (68) is taken as a square function activated at $t = 2$ and deactivated at $t = 7$. Figure 17 shows the reconstruction result of the estimated output using $N_C = N_0 = 3$.

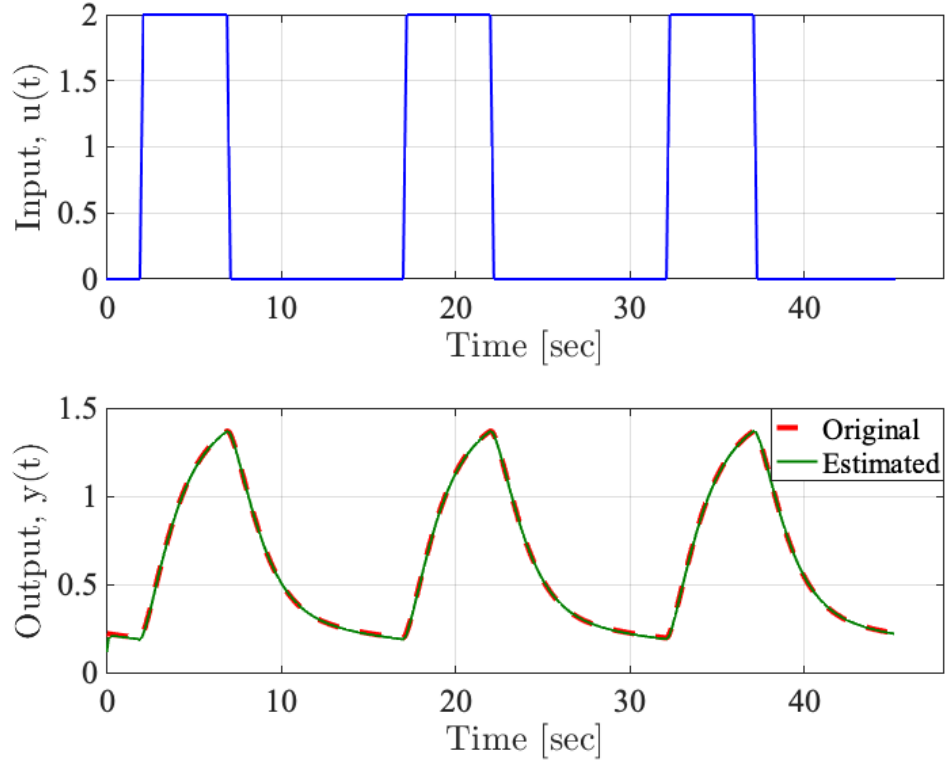


Figure 17: Estimated output signal along with the real one using random input signal. Here we use $N_0 = 3$ and $N_C = 15$.

The relative errors of the unknown parameters $(a_1, a_2, \alpha_1, \alpha_2)$ are (4.19%, 4.17%, 1.07%, 5.84%) respectively and for the reconstructed output is 0.86%. It is clear in this example that although the percent relative error of the reconstructed output is very low, the relative errors of the unknown parameters and fractional differentiation estimates are higher. This can be explained by the fact that fractional-order systems with more than one fractional differentiation order are not structurally globally identifiable [29]. Figure 18 shows the percent relative errors of the estimation of the parameters $(a_1; a_2)$, the fractional differentiation orders $(\alpha_1; \alpha_2)$ and the reconstructed output $y(t)$. Based on these results, overall, we have a good reconstruction. In all cases, the percent relative error does not exceed 3%. The best performance is achieved with large values of N_C and N_0 . Concerning the

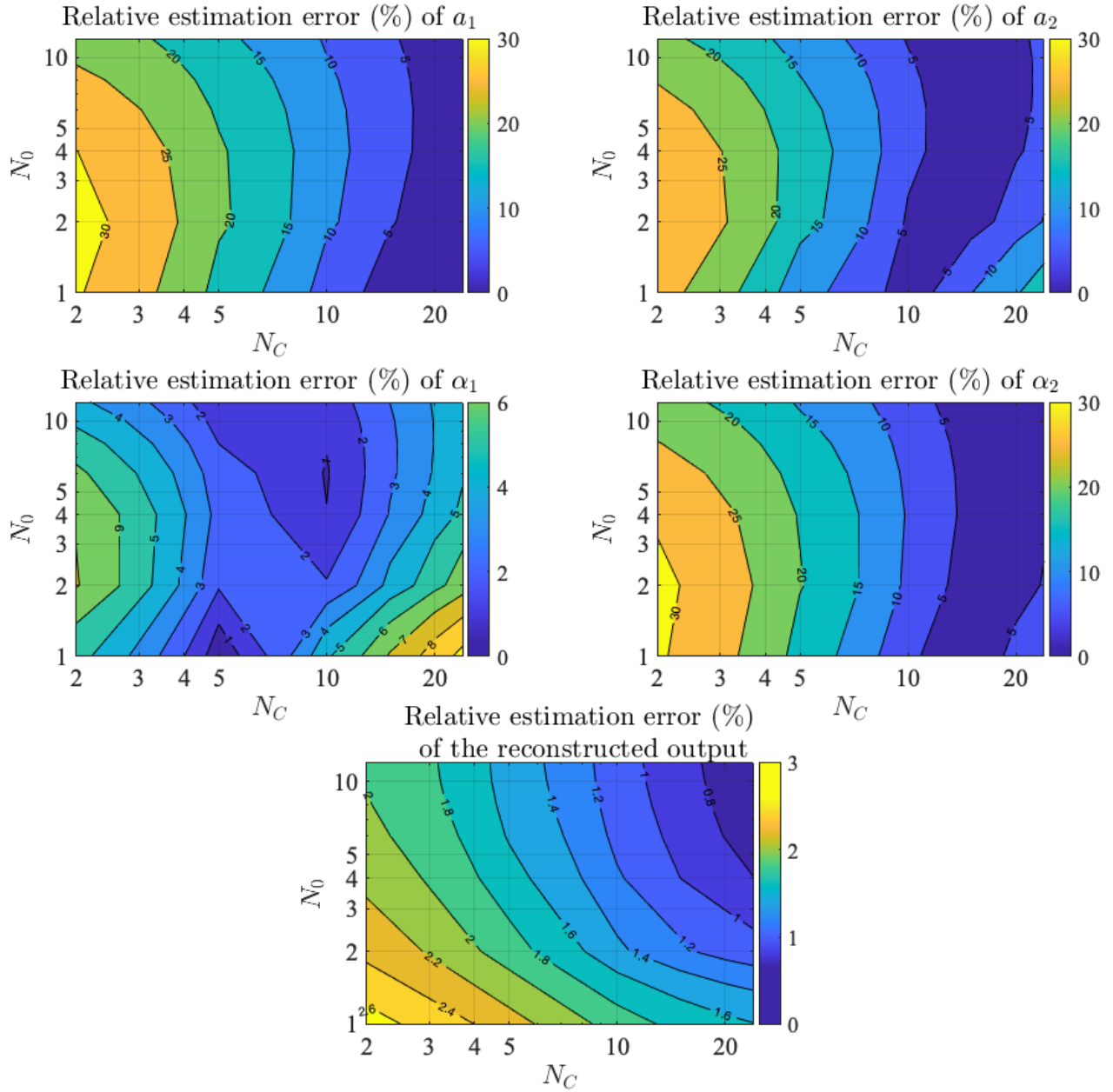


Figure 18: Contour plot of the relative error (%) with respect to N_C and N_0 for parameters, fractional differentiation orders and the reconstructed output signal. The sampling rate $h = 0.01$ has been used in this simulation.

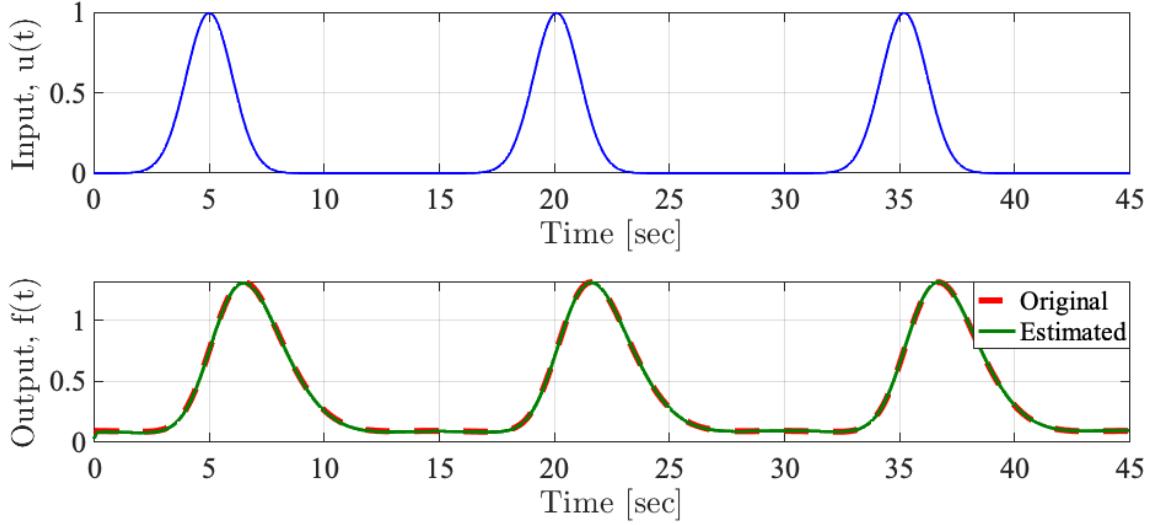


Figure 19: Estimated output signal along with the real one using random input signal. Here we use $N_0 = 3$ and $N_C = 10$.

parameters and fractional differentiation orders, we obtained the same aspect. However, the error is larger than the ones obtained in the reconstruction of the output.

7.2.3 Joint estimation of the parameters and the fractional differentiation order for a fractional neurovascular mode

A potential application of the proposed method is to estimate the neural activity and the fractional differentiation orders from the Cerebral Blood Flow (CBF) measurements. In [30], a fractional model for the neurovascular coupling in the brain has shown a better characterization of the cerebral hemodynamic response. This model relates the neural activity, considered as input, to the CBF considered as output. To fully identify the fractional neurovascular model, the input and the fractional differentiation orders have to be estimated from CBF data. The nature of the neural activity can be of two types: the block design paradigm, which corresponds to tasks lasting for extended periods of time, and the event-related paradigm, which corresponds to tasks lasting for shorter periods. This

section focuses on estimating the event-related type of neural activity usually modeled by Gaussian functions. The neurovascular model is given as follows:

$$D_t^{\alpha_1} f(t) + k D_t^{\alpha_2} f(t) + \gamma f(t) = u(t), \quad t \in [0, 15] \quad (70)$$

where $1 \leq \alpha_1 \leq 2$, $0 \leq \alpha_2 \leq 1$ are the fractional differentiation orders, $f(t)$ is the temporal CBF and $u(t)$ is the temporal neuronal activity. The constants k and γ are the flow signal decay rate and the flow-dependant elimination constant, respectively. Their values are given in as: $k = 0.65$, $\gamma = 0.41$.

The tested input profile is Gaussian which can be expressed as:

$$u(t) = \exp \left[-(t - 5)^2 \right] \quad (71)$$

We use a synthetic data set which have been generated from discretizing the neurovascular model (70) and fixing $\alpha_1 = 1.7, \alpha_2 = 0.6$.

Figure 19 shows the reconstruction result of the estimated output using $N_C = 10$ and $N_0 = 3$. The relative errors of the unknown parameters ($k, \gamma, \alpha_1, \alpha_2$) are (1.32%, 1.64%, 0.62%, 1.67%) respectively and for the reconstructed output is 0.57%.

In figures 20, we summarize the results of the relative errors of the estimated unknown parameters, fractional differentiation orders, and the reconstructed output for a different combination of $(N_0; N_C)$. From these results, it is clear that as the N_C increases the estimation accuracy increases. It is worth noting that for a small value of N_C increasing N_0 enhances the estimation accuracy.

8 Conclusion

The concept of initialized fractional calculus is of great pertinence for the uniqueness of solutions to fractional forward problems. This report investigates their significance for solving inverse problems.

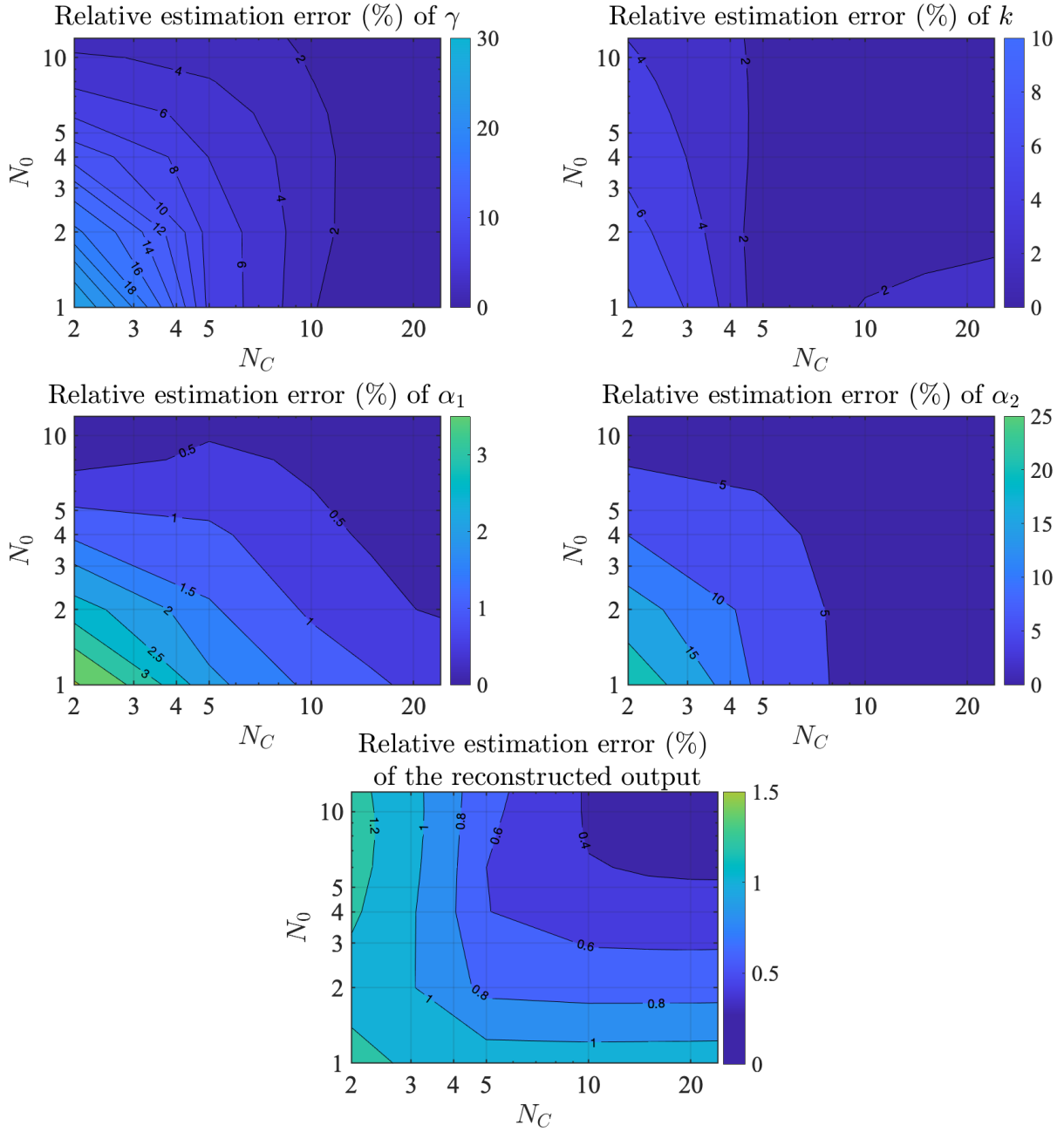


Figure 20: Contour plot of the relative error (%) with respect to N_C and N_0 for parameters, fractional differentiation orders and the reconstructed output signal. The sampling rate $h = 0.1$ has been used in this simulation.

We proposed an initialized estimation algorithm to jointly estimate the parameters and the fractional differentiation orders while designing an output-dependent history function based-initialization. After reformulating the estimation problem in the discrete space, we proposed an algorithm of two steps that study the effect of the length of the initialization function while estimating the unknown parameters. We applied the pipeline to different numerical examples. Furthermore, potential applications of the proposed algorithm are presented, which consists of joint estimation of parameters and fractional differentiation orders of a fractional-order arterial Windkessel and neurovascular models. In future work, we will propose a multi-stage estimation algorithm based on modulating functions that are known to be robust to noise.

References

- [1] R. Gorenflo and F. Mainardi, “Fractional calculus,” in *Fractals and fractional calculus in continuum mechanics*. Springer, 1997, pp. 223–276.
- [2] R. L. Magin, “Fractional calculus models of complex dynamics in biological tissues,” *Computers & Mathematics with Applications*, vol. 59, no. 5, pp. 1586–1593, 2010.
- [3] R. Matusu, “Application of fractional order calculus to control theory,” *International journal of mathematical models and methods in applied sciences*, vol. 5, no. 7, pp. 1162–1169, 2011.
- [4] V. E. Tarasov, “On history of mathematical economics: Application of fractional calculus,” *Mathematics*, vol. 7, no. 6, p. 509, 2019.
- [5] I. Podlubny, “Fractional-order systems and fractional-order controllers,” *Institute of Experimental Physics, Slovak Academy of Sciences, Kosice*, vol. 12, no. 3, pp. 1–18, 1994.

- [6] C. F. Lorenzo and T. T. Hartley, “Initialization of fractional-order operators and fractional differential equations,” *Journal of computational and nonlinear dynamics*, vol. 3, no. 2, 2008.
- [7] M. A. Bahloul, Z. Belkhatir, and T.-M. L. Kirati, “Initialization of fractional order systems for the joint estimation of parameters and fractional differentiation orders,” in *2022 American Control Conference (ACC)*. IEEE, 2022, pp. 3943–3948.
- [8] G. B. H. Frej, R. Malti, M. Aoun, and T. Raissi, “Fractional interval observers and initialization of fractional systems,” *Communications in Nonlinear Science and Numerical Simulation*, vol. 82, p. 105030, 2020.
- [9] H. Ye and R. Huang, “Initial value problem for nonlinear fractional differential equations with sequential fractional derivative,” *Advances in Difference Equations*, vol. 2015, no. 1, pp. 1–13, 2015.
- [10] C. F. Lorenzo and T. T. Hartley, “Initialization in fractional order systems,” in *2001 European Control Conference (ECC)*. IEEE, 2001, pp. 1471–1476.
- [11] —, “Initialization, conceptualization, and application in the generalized (fractional) calculus,” *Critical ReviewsTM in Biomedical Engineering*, vol. 35, no. 6, 2007.
- [12] B. Du, Y. Wei, S. Liang, and Y. Wang, “Estimation of exact initial states of fractional order systems,” *Nonlinear Dynamics*, vol. 86, no. 3, pp. 2061–2070, 2016.
- [13] D. Liu, T. M. Laleg-Kirati, O. GIBARU, and W. Perruquetti, “Identification of fractional order systems using modulating functions method,” in *2013 IEEE American Control Conference*. IEEE, 2013.

- [14] Z. Belkhatir and T. M. Laleg-Kirati, “Joint estimation of the fractional differentiation orders and the unknown input for linear fractional non-commensurate system,” in *2015 IEEE Conference on Control Applications (CCA)*. IEEE, 2015, pp. 388–393.
- [15] —, “Parameters and fractional differentiation orders estimation for linear continuous-time non-commensurate fractional order systems,” *Systems & Control Letters*, vol. 115, pp. 26–33, 2018.
- [16] M. A. Bahloul, M. Benencase, Z. Belkhatir, and T.-M. L. Kirati, “Finite-time simultaneous estimation of aortic blood flow and differentiation order for fractional-order arterial windkessel model calibration,” *IFAC-PapersOnLine*, vol. 54, no. 15, pp. 538–543, 2021.
- [17] S. Das, “Initialized differintegrals and generalized calculus,” in *Functional Fractional Calculus*. Springer, 2011, pp. 271–322.
- [18] K. Diethelm, *The analysis of fractional differential equations: An application-oriented exposition using differential operators of Caputo type*. Springer Science & Business Media, 2010.
- [19] M. Ö. Efe, “Fractional order systems in industrial automation—a survey,” *IEEE Transactions on Industrial Informatics*, vol. 7, no. 4, pp. 582–591, 2011.
- [20] C. F. Borges, “A full-newton approach to separable nonlinear least squares problems and its application to discrete least squares rational approximation,” *Electronic Transactions on Numerical Analysis*, vol. 35, pp. 57–68, 2009.
- [21] T. Kurmayya and K. Sivakumar, “Moore-penrose inverse of a gram matrix and its nonnegativity,” *Journal of optimization theory and applications*, vol. 139, no. 1, pp. 201–207, 2008.
- [22] C. T. Kelley, *Iterative methods for linear and nonlinear equations*. SIAM, 1995.

- [23] M. A. Bahloul and T.-M. Laleg-Kirati, "Assessment of fractional-order arterial windkessel as a model of aortic input impedance," *IEEE Open Journal of Engineering in Medicine and Biology*, vol. 1, pp. 123–132, 2020.
- [24] T. M. Laleg and M. A. Bahloul, "Mathematical biomarker for arterial viscoelasticity assessment," Nov. 18 2021, uS Patent App. 17/284,072.
- [25] M. A. Bahloul, Y. Aboelkassem, and T.-M. Laleg-Kirati, "Human hypertension blood flow model using fractional calculus," *Frontiers in Physiology*, vol. 13, p. 838593, 2022.
- [26] —, "Towards characterization of the complex and frequency-dependent arterial compliance based on fractional-order capacitor," in *2021 43rd Annual International Conference of the IEEE Engineering in Medicine & Biology Society (EMBC)*. IEEE, 2021, pp. 5559–5565.
- [27] S. Bernhard, K. Al Zoukra, and C. Schtte, "From non-invasive hemodynamic measurements towards patient-specific cardiovascular diagnosis," in *Quality Assurance in Healthcare Service Delivery, Nursing and Personalized Medicine: Technologies and Processes*. IGI Global, 2012, pp. 1–25.
- [28] P. H. Charlton, J. Mariscal Harana, S. Vennin, Y. Li, P. Chowienczyk, and J. Alastruey, "Modeling arterial pulse waves in healthy aging: a database for in silico evaluation of hemodynamics and pulse wave indexes," *American Journal of Physiology-Heart and Circulatory Physiology*, vol. 317, no. 5, pp. H1062–H1085, 2019.
- [29] S. Alavi, A. Mahdi, P. E. Jacob, S. J. Payne, and D. A. Howey, "Structural identifiability analysis of fractional order models with applications in battery systems," *arXiv preprint arXiv:1511.01402*, 2015.

- [30] Z. Belkhatir and T. M. Laleg-Kirati, “Fractional dynamical model for neurovascular coupling,” in *2014 36th Annual International Conference of the IEEE Engineering in Medicine and Biology Society*. IEEE, 2014, pp. 4916–4919.